Int J Earth Sci (Geol Rundsch) (2003) 92:114–142
DOI 10.1007/s00531-002-0304-9

ORIGINAL PAPER

**P. Schulte · W. Stinnesbeck · D. Stüben · U. Kramar · Z. Berner · G. Keller · T. Adatte**

# Fe-rich and K-rich mafic spherules from slumped and channelized Chicxulub ejecta deposits in the northern La Sierrita area, NE Mexico

Received: 2 October 2001 / Accepted: 22 August 2002 / Published online: 13 February 2003


**Abstract** Spherule deposits, commonly interpreted as ejecta from the Chicxulub impact at Yucatán, Mexico, are present in many K-T (Cretaceous-Tertiary) sections. Geological mapping of the northern La Sierrita area, NE Mexico, revealed the presence of (1) multiple spherule deposits embedded in late Maastrichtian marls, which are folded or disaggregated (breccia-like). They are up to 6 m thick, locally present in two outcrop areas, and show limited lateral continuity. These deposits consist of mm–cm sized spherical to drop-shaped vesiculated spherules, angular to filamentous (ejecta-) fragments and abundant carbonate. They are interpreted as primary ejecta fallout deposits that have been affected by subsequent local slumps-slides, liquefaction, and debris flows; welded components suggest an initial ground surge-like ejecta-dispersion mode. (2) A spherule deposit, 10–60 cm thick that constitutes the base of a channelized sand-siltstone deposit at, or close to, the K-T boundary and is characterized by wide lateral continuity. It is of similar petrologic composition to deposit (1), though slightly enriched in terrigeneous detritus, thus reflecting influx from proximal shelf areas. It is interpreted to result from debris flows and turbidite currents, though no size sorting and abrasion of ejecta has been observed. Petrological, mineralogical, and geochemical criteria suggest that ejecta components from both types of spherule deposits are similar and originated from the Chicxulub impact, with multiple deposits produced by subsequent remolding, reworking, and redeposition. Spherules and fragments have an Fe- (25–30 wt%), Al-, Mg-rich and Si-poor (<25 wt% $SiO_2$) composition, and are altered to chlorite and iron-oxides, though rare K-rich mafic glass (~50 wt% $SiO_2$; 5–8 wt% K) is also present. They contain Ti-, Fe-, K-rich schlieren, Fe-, Mg-rich globules, and rare μm-sized metallic and sulfidic Ni-, Co-rich inclusions. Carbonate as clasts and within spherules and fragments shows textures indicative of quenching and/or liquid immiscibility. Although potential ejecta fractionation and alteration make accurate evaluation difficult, this composition suggests an ejecta origin mainly from mafic lithologies and carbonaceous sediments, in addition to a contribution from intermediate felsic rocks and the possibility of meteoritic contamination.

**Keywords** Mexico · K-T boundary · Chicxulub · Ejecta · Spherules · Iron-rich · Mafic composition

P. Schulte (✉) · W. Stinnesbeck
Geologisches Institut, Universität Karlsruhe,
Postfach 6980, 76128 Karlsruhe, Germany
e-mail: peter.schulte@bio-geo.uni-karlsruhe.de
Tel.: +49-721-6082943
Fax: +49-721-6082138

D. Stüben · U. Kramar · Z. Berner
Institut für Mineralogie und Geochemie,
Universität Karlsruhe, 76128 Karlsruhe, Germany

G. Keller
Department of Geosciences, Princeton University,
Princeton, New Jersey, 08544, USA

T. Adatte
Institut de Géologie, Université de Neuchâtel,
2007 Neuchâtel, Switzerland

## Introduction

Spherules are a salient component of many localities that contain the Cretaceous–Tertiary (K-T) boundary worldwide (e.g., Ryder et al. 1996; Smit 1999; Montanari and Koeberl 2000; Claeys et al. 2002). These spherules are generally interpreted to be of impact ejecta origin and are ascribed to the Chicxulub impact on the Yucatán peninsula, Mexico (e.g., Izett 1991; Smit et al. 1992b; Bohor and Glass 1995; Martínez-Ruíz et al. 1997; Claeys et al. 2002). In this context, ejecta formations, such as spherule deposits and their spatial distribution, lithology, and degree of shock metamorphism are instrumental in determining pre-impact target lithology, extent of excavation, trajectory of the projectile, and P/T conditions during the impact (e.g., Melosh 1989; Engelhardt et al. 1997; Pierazzo and Melosh 1999; Kettrup et al. 2000; Montanari and Koeberl 2000). This information is crucial for estimating the amounts of water, carbonate, sulfate,

**Table 1** Published occurrences and compositional characteristics of selected "type 1" spherule deposits in Central and North America and adjacent areas. Spherules from these sections are morphologically similar to spherules in the La Sierrita area (e.g. in grain-size, shape, internal textures); see also the overview in Claeys et al. (2002)

| Region | Location/Site | References[a] | Spherules | Carbonate clasts | Shocked quartz | Mineralogy of spherules | Grain-size (mm) | |
|---|---|---|---|---|---|---|---|---|
| | | | | | | | Mean | Max. |
| Terrestrial continental North America | | | | | | | | |
| Montana, Wyoming, Colorado | Hell Creek, Dogie Creek, Sussex, Lance Creek, Teapot Dome, Raton Basin | 1 | X | – | X | Kaolinite, goyazite | 0.5–1 | ~1 |
| Marine setting | | | | | | | | |
| New Jersey | ODP 174AX | 2 | X[b] | X | X | "Clay" | 0.2–1 | ~1.1 |
| Bermuda Rise | DSPD 386 | 3 | X | X | X | Smectite, chlorite, glauconite | 0.5–1 | ~1.5 |
| Blake Plateau | ODP 171 | 4 | X | X | X | Smectite | - | ~3 |
| Alabama | Moscow Landing, Shell Creek | 5 | X | X | – | "Clay" | 2–3 | 3 |
| Texas | Brazos River | 6 | X | X | – | Smectite, glauconite | 1 | ~2 |
| Haiti | Beloc | 7 | X | X | X | Glass, smectite, palagonite | 1.2 | ~8 |
| Caribbean Sea | ODP 165 | 8 | X[b] | X | X | "Clay" | 1.5 | 2 |
| Belize | Albion Island | 9 | X | X | X | Smectite, palagonite | 3 | ~10 |
| NE Mexico | El Peñon, La Lajilla, El Mimbral | 10 | X | X | X | Chlorite, chlorite-smectite, illite, glass, smectite, zeolite | 1.5 | ~8 |
| NE Mexico | La Sierrita | This study | X | X | – | Chlorite, chlorite-smectite, illite, glass, smectite, zeolite | 1.2 | ~10 |

[a] 1, Bohor et al. (1987); Izett (1990); Schmitz (1992); Pollastro and Bohor (1993); Bohor and Glass (1995); Sweet et al. (1999;) Sweet (2001); 2, Olsson et al. (1997, 2002); 3, Klaver et al. (1987); Bohor and Betterton (1989); Norris et al. (2000); 4, Norris et al. (1999); Martínez-Ruíz et al. (2001a, 2001b); (2002); 5, Pitakpaivan et al. (1994); Smit et al. (1996); 6, Smit et al. (1996); Yancey (1996); 7, Izett (1991); Koeberl and Sigurdsson (1992); Bohor and Glass (1995); Stüben et al. (2002); 8, Sigurdsson et al. (1997); 9, Pope et al. (1999); 10, Premo et al. (1995); Adatte et al. (1996); Smit et al. (1996); Stinnesbeck et al. (1996)

[b] Indicates poor preservation of morphological details

and dust released by the impact that are required for modeling the resulting environmental and climatic effects of this event (Covey et al. 1994; Ivanov et al. 1996; Pope et al. 1997; Toon et al. 1997; Pierazzo et al. 1998; Gupta et al. 2001). Accurate knowledge of these perturbations is necessary for evaluating the significance of the Chicxulub impact within the entirety of events (e.g., Deccan volcanism), and environmental changes (e.g., climate cooling) that took place during the K-T transition and presumably contributed to the biological crisis at the end of the Cretaceous period (e.g., Keller 1996; MacLeod et al. 1997; Toon et al. 1997; Barrera and Savin 1999; Hallam and Wignall 1999; Wignall 2001; Kiessling and Claeys 2001). In addition, impactoclastic layers may document the mechanisms of ejecta dispersion and deposition, as well as later reworking (Smit et al. 1996; Smit 1999; McHugh et al. 1998; Tsikalas et al. 1998; Ormö and Lindström 2000; Sturkell et al. 2000).

## Characteristics of spherule deposits

In K-T sections from the Caribbean to the Western Interior and from southern Mexico to the western Atlantic (Table 1, Fig. 1), morphology of the mm–cm sized spherules is spherical to teardrop-shaped, including forms with internal textures, such as vesicles and schlieren (e.g., Izett 1991; Bohor and Glass 1995; Smit 1999). This classifies them as "type 1" spherules that are interpreted to have originated as glassy fallout ("microtektites") from the impact ejecta curtain, but are now altered to clay minerals (e.g., smectite), or intermediate phases (e.g., palagonite), with schlieren-rich glass cores of andesitic composition (e.g., Izett 1991; Sigurdsson et al. 1991; Bohor and Glass 1995; Premo et al. 1995; Martínez-Ruíz et al. 2002; Claeys et al. 2002). In contrast, "type 2" spherules are solid, in part Ni-, Cr-spinel-bearing "microcrysts" of either K-feldspar, Fe-oxide, or smectite composition and are confined to the "red" siderophile- and platinum group-element (PGE) enriched K-T boundary clay from the Atlantic, Pacific, and Tethyan realm (Smit and Klaver 1981; Doehne and Margolis 1990; Montanari 1991; Bohor and Glass 1995; Martínez-Ruíz et al. 1997; Ortega-Huertas et al. 1998; Bauluz et al. 2000; Wdowiak et al. 2001; Claeys et al. 2002). These microcrysts and the boundary clay presumably formed by condensation from vaporized target-rock and meteoritic materials in the expanding fireball.

Sections encompassing the K-T boundary in the Western Interior of North America comprise a cm-thick two-layer sequence in a terrestrial setting (see Table 1 with references): a lower "type 1" spherule-rich layer with rare shocked minerals directly underlies a laminated clay layer rich in shocked minerals, iridium, siderophile elements, and Ni-rich spinels. According to palynological studies (Lerbekmo et al. 1999; Sweet et al. 1999; Sweet 2001), these two layers are separated by a "microdiastem" and represent the initial melt-ejecta, followed by


**Fig. 1** Gulf of Mexico with adjacent areas and K-T boundary sections referred to in this study. Note that these sections comprise "type 1" spherules, whereas "type 2" spherules are found in K-T sections in the Atlantic, Pacific and Tethyan realm (see text and Table 1 for details and references)

fallout from stratospherically and globally dispersed ejecta (Alvarez et al. 1995; Bohor and Glass 1995).

The K-T boundary present in marine sections in the Gulf of Mexico and adjacent areas comprises "type 1 spherule" deposits, associated with carbonate clasts and shocked quartz (Table 1, Fig. 1). At the New Jersey coastal plane, western Atlantic (ODP Leg 174AX), a thin spherule layer interpreted as an original in-situ ejecta fallout deposit separates lowermost Danian (*P. eugubin*a zone P1a) from uppermost Maastrichtian sediments (Olsson et al. 1997; 2002). Three cores from the Blake Nose Plateau, western Atlantic (ODP Leg 171B) include a reworked spherule deposit that overlies disturbed uppermost Maastrichtian sediments and underlies sediments of early Paleocene age (*P. eugubin*a zone P1a), thus documenting large-scale slumping that preceded deposition and remobilization of ejecta (Norris et al. 1999; 2000; Klaus et al. 2000; MacLeod and Huber 2001; Martínez-Ruíz et al. 2001a; 2001b; 2002). Spherule deposits in the Brazos river (Texas) sections are at the base of a siliciclastic complex that lies at, or close to, the K-T boundary (Bourgeois et al. 1988; Keller 1989; Hansen et al. 1993; Smit et al. 1996), and contains evidence for reworking by successive debris flows and turbidites (Yancey 1996; Smit et al. 1996; Heymann et al. 1998). Multiple spherule deposits in early Danian (*P. eugubin*a zone P1a) sediments at Beloc, Haiti (Stinnesbeck et al. 1999; Keller et al. 2001), indicate that these spherules have been reworked, probably by turbidites, whereas other sections indicate subsequent slumping, faulting, and thrusting (Maurrasse and Sen 1991; Lyons and Officer 1992; Stinnesbeck et al. 1999; Keller et al. 2001). In two cores of the Caribbean, ODP Leg 165, Site 1001, one

single graded spherule deposit overlies upper Maastrichtian sediments and underlies earliest Paleocene sediments (*P. eugubin*a zone P1a) (Sigurdsson et al. 1997). In NE Mexico, sections spanning more than 300 km include an up to 60-cm-thick spherule deposit at the base of a channelized 'siliciclastic deposit' which underlies the K-T boundary (Stinnesbeck et al. 1993; Smit et al. 1992b; 1996). This 'siliciclastic deposit' has been interpreted as a short-term Chicxulub impact-triggered megatsunami or gravity flow deposit (e.g., Smit et al. 1992b; 1996; Smit 1999; Bohor 1996; Arz et al. 2001; Alegret et al. 2001). Alternatively, it has been interpreted as long-term sea-level lowstand deposit (e.g., Stinnesbeck et al. 1993; 1996; Keller et al. 1997; Ekdale and Stinnesbeck 1998).

Recent geological mapping of sediments across the K-T boundary in the La Sierrita area of northeastern Mexico by two teams from the University of Neuchâtel, Switzerland (Affolter 2000; Schilli 2000) and the University of Karlsruhe, Germany (F. Lindenmaier, C. Ifrim, and P. Schulte) revealed the local presence of spherule deposits in hemipelagic marls of latest Maastrichtian age, in part with sedimentary deformation structures, in addition to the common presence of a spherule layer at the base of the 'siliciclastic deposit' (Stinnesbeck et al. 2001; Keller et al. 2002a; 2002b). These deposits show pristinely preserved microfacies characteristics, extraordinary iron-rich, as well as K-rich mafic ejecta compositions, and abundance of carbonate clasts. In this study, we report the results of a multidisciplinary investigation in the area to the north of La Sierrita that (1) documents the spatial and stratigraphic distribution of the various spherule deposits, (2) examines their sedimentological and petrological characteristics, and (3) analyzes their mineralogical and geochemical composition. The primary objectives are: (1) to evaluate the origin of the spherules and their initial dispersion mode and (2) to distinguish between the sedimentary processes that originated these deposits. For details on the biostratigraphic position of these deposits in the La Sierrita area with respect to the K-T boundary, the reader is referred to the discussion provided by Soria et al. (2001, 2002), Stinnesbeck et al. (2001), and Keller et al. (2002a, 2002b).

## Methodology

During geological mapping, samples were collected from spherule deposits, marls, and sandstones. About 200 thin sections were analyzed petrographically. Marls and spherule-deposits were prepared for biostratigraphic analysis after methods given by Keller et al. (1997). For the geochemical and mineralogical analyses, samples were dried, crushed, and finely ground in an agate mill.

Bulk rock and clay mineralogy were analyzed by X-ray diffractometry (XRD) at the Geological Institute of the University of Neuchâtel, Switzerland, with a SCINTAG XRD 2000 diffractometer and Cu-k$\alpha$ radiation. Diffractograms were evaluated with the MacDIFF software (freeware by R. Petschick, University of Frankfurt) and methods outlined in Moore and Reynolds (1997). For bulk rock samples, the relative abundance of the dominant nonclay minerals quartz, feldspar, and calcite was estimated by using the intensity of their main diffraction peak. Methods for the semi-quantitative clay mineral analysis of the insoluble residue (<2 μm) are described in Adatte et al. (1996).

Major elements were determined by wavelength-dispersive X-ray fluorescence spectrometry (WDS) at the Institute for Mineralogy and Geochemistry, University of Karlsruhe, with a SRS 303 AS XRF. For these analyses, fused glass discs were prepared from a mixture of 1 g ignited powder of each sample and 4 g of SPECTROMELT. Trace elements (Cr, Ni, Cu, Zn, As, Rb, Sr, Y, Zr, Ba, La, Ce, and Pb) were analyzed from bulk powder samples (5 g) by energy-dispersive X-ray fluorescence spectrometry (EDS) with a SPECTRACE 5000 X-ray analyzer. Detailed analytical procedures and the standards used were compiled by Kramar (1997); detection limits are given in Table 5.

Wavelength-dispersive (WDS) and energy-dispersive (EDS) electron microprobe analyses, as well as back-scattered electron (BSE) images were performed with a CAMECA SX50 microprobe on polished thin sections at the Laboratory for Electron Microscopy, University of Karlsruhe. All quantitative major element analyses were calibrated with the following standards: Fe:$Fe_2O_3$; Si:wollastonite; Mg:MgO; K:orthoclase; Ca, Al:anorthite; Ti:$MnTiO_3$; Na:albite; Ni:NiO. The accelerating voltage was set to 15–20 kV and counting times of 120–200 s were used. Detection limits are in the range between 0.5 and 1 wt‰.

## Spherule deposits in the northern La Sierrita area

### Locations and geological setting

The La Sierrita area is situated in the Gulf-coastal plain of northeastern Mexico in the state of Nuevo León, 80 km southeast of Monterrey and 40 km east of Montemorelos (Fig. 1). For this study, an area of 20 $km^2$ to the north of La Sierrita was geologically mapped (Fig. 2). The outcrops are located on the flanks of NW–SE trending low-lying hills near the small hamlet of La Sierrita and to the south and north of the road that connects General Terán and Vaquerías (Fig. 2a). The slopes of these hills consist of uniform gray to olive-green marls of the Maastrichtian Méndez Formation. At two outcrop localities, spherule deposits are interbedded in these marls (as outlined below, Figs. 3, 4). Biostratigraphic analysis of the topmost 1–5 m of the Méndez marls in several sections (marked with an asterisk in Fig. 4) revealed the presence of *P. hantkeninoides* (zone CF1). This indicates deposition of these Méndez marls during the last 200–300 ka of the Maastrichtian (Pardo et al. 1996; Li and Keller 1998). Studies by Alegret et al. (2001), Soria et al. (2001), and Keller et al. (2002b) on benthic foraminifera

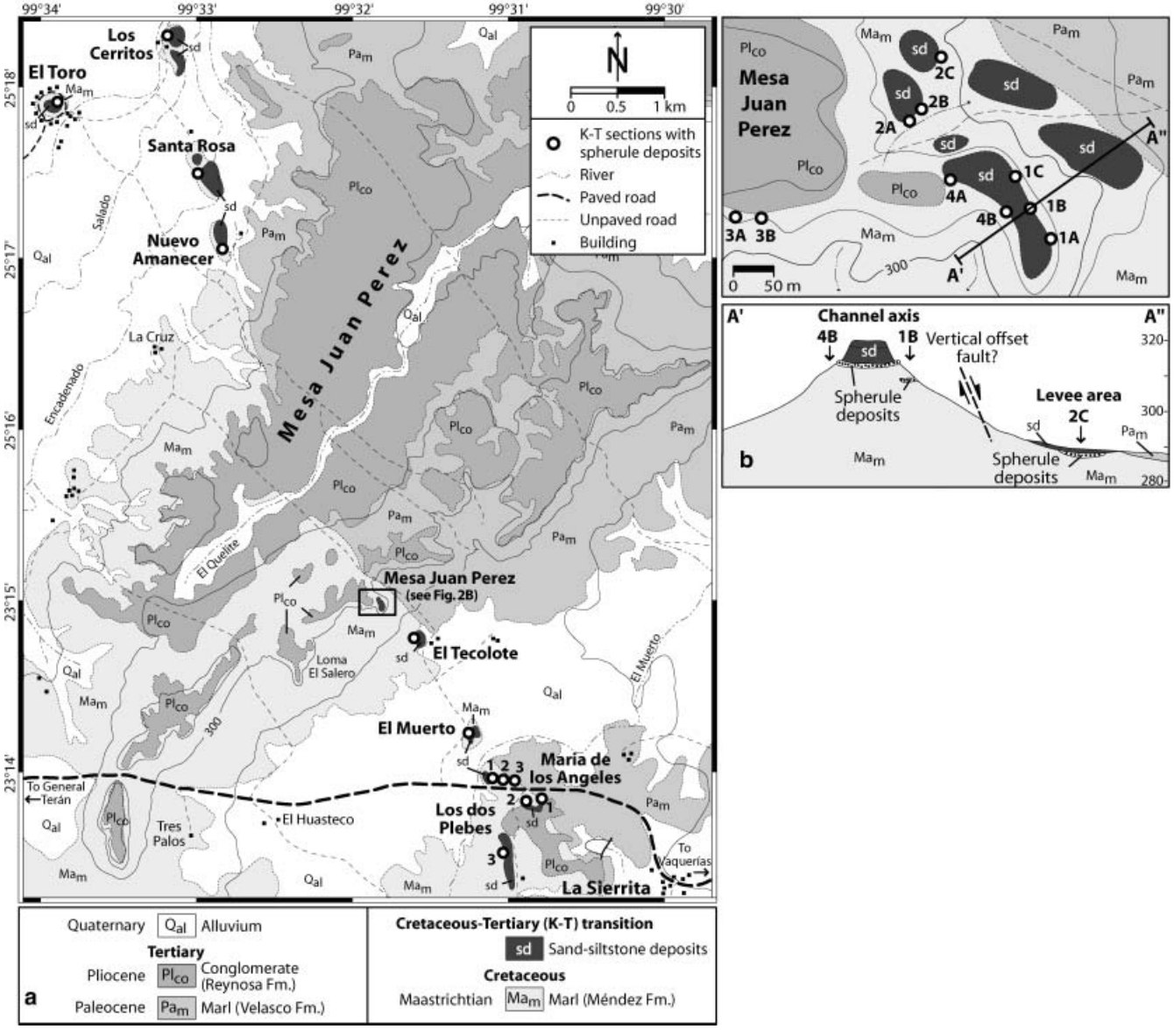


**Fig. 2** **a** Geological map of the La Sierrita area with K-T sections examined herein. It reveals the channel-like lateral persistence of the NNW/SSE-trending sand-siltstone complex, with exception of the El Toro section that is found about 0.5 km to the west of the main channel axis. General dip of the units is towards NEE (about 5–10°). Note that sections with spherule deposits embedded in Méndez marls have only been found in two outcrop areas at the Mesa Juan Perez and at Maria de los Angeles in contrast to the wide distribution of the unit 1 spherules deposit. **b** A close-up of the Mesa Juan Perez area with the sections examined (*upper illustration*) and a crosscut (A'–A3, *below*), revealing the spatial and stratigraphic relationships of spherule- and sand-siltstone deposits. Note lateral discontinuity of spherule deposits within Méndez marls and vertical offset of spherule-sandstone deposits by postsedimentary faulting. A similar offset of the sand-siltstone complex (>10 m) was observed at the Maria de los Angeles area

suggest that sediment deposition occurred in an upper slope to middle bathyal environment at a water depth of about 300–1,000 m.

Overlying the Méndez marls, a prominent sand-siltstone deposit marks the top of these hills (Figs. 2, 3, 4); it has a channel-like geometry with an apparent low sinuosity (trend of channel axis ~170°) and a dip of 5–10° to NE. The channel levee complex is generally dislocated relative to the channel axis and shows a vertical offset of up to ten meters (Fig. 2b). The sand-siltstone deposits in the La Sierrita area are characterized by three distinct units: (1) a basal spherule deposit (unit 1, see below). (2) The overlying unit 2 is 0.5–8 m thick laminated sandstone that consists of quartz (30–40 vol%), carbonate clasts (20–30 vol%), and feldspar (10–15 vol%), and contains large marl clasts, plant debris, and rare spherules at the base. With the exception of one 25-cm-long, J-shaped burrow in the Mesa Juan Perez 1B section, no bioturbation was observed in this unit. (3) The topmost unit 3 presents 0.1–1.5 m thick alternating silt-sandstones with similar composition as unit 2, but with abundant foraminifera tests (up to 40 vol%). Its top is orange-

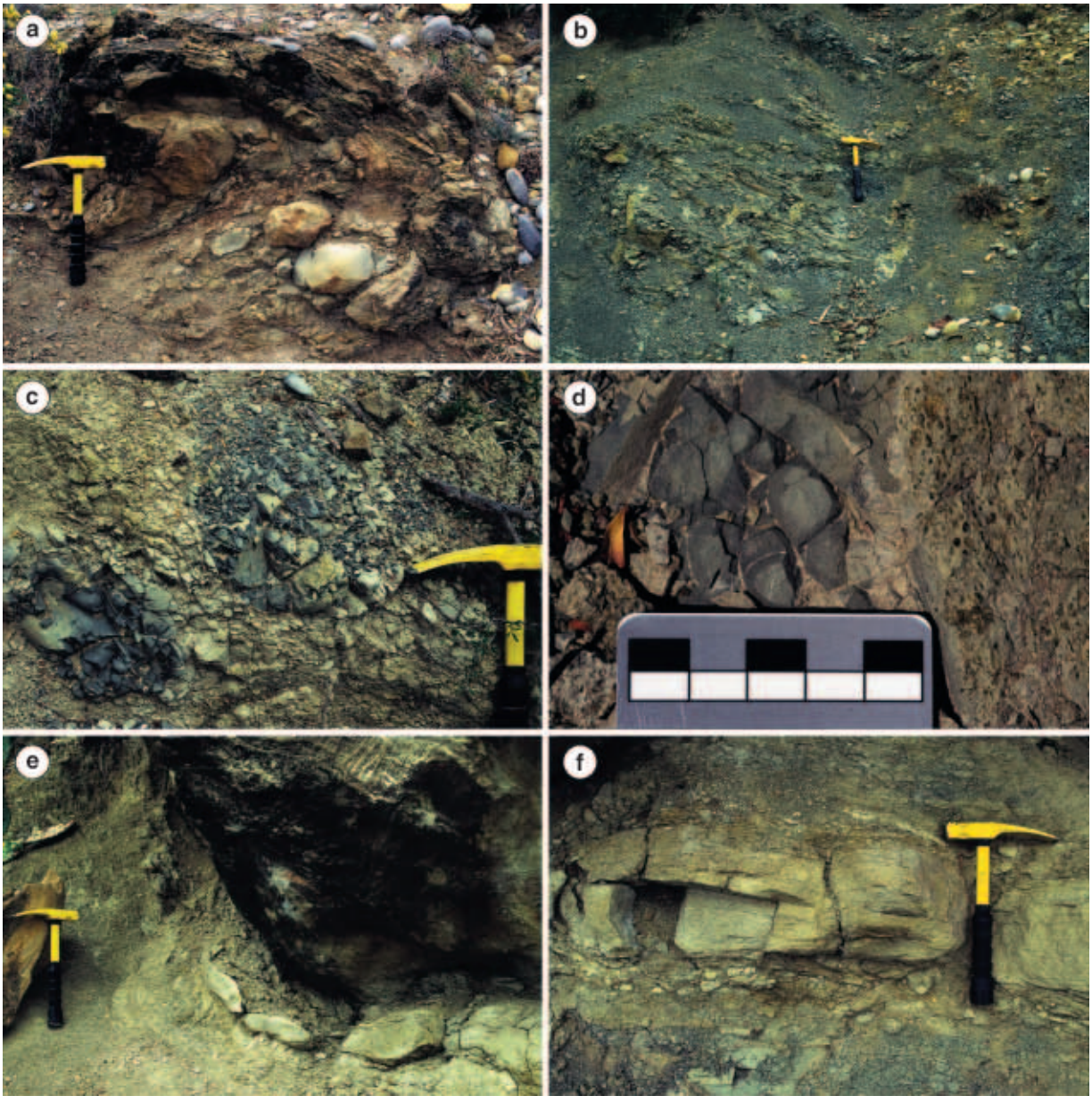


**Fig. 3a–f** Photos of sections in the La Sierrita area with details of the spherule deposits; hammer as scale (30 cm). **a** Recumbent folded spherule deposit with large marl clasts in the core of the fold in the Mesa Juan Perez 3A section. The axis of the slump fold has a northeastern trend and the fold is open towards southeast. **b** 'Breccia-like' marl and spherule deposits in the Mesa Juan Perez 3B section. **c** and **d** show squeezing and mixing of spherule deposits with Méndez marl at the Mesa Juan Perez 2A section, interpreted as slump-slide or liquefaction structures. **e** Unit 1 at the base of the sand-siltstone deposit in the Mesa Juan Perez 1A section with boudinage structures and lateral pinching out of the indurated calcareous spherule layer. **f** Close-up from **a** showing alternating layers of weathered marl and spherule layers under- and overlying the indurated calcareous spherule layer

stained, rippled, and bioturbated by *Chondrites*, *Planolites*, and *Ophiomorpha*. Similar sand-siltstone units, though with variable thickness, petrological composition, and amount of bioturbation have been reported from a number of K-T sections in NE Mexico (e.g., El Peñon, La Lajilla, El Mimbral, see Fig. 1; Smit et al. 1992b, 1996; Stinnesbeck et al. 1993, 1996; Keller et al. 1994, 1997; Soria et al. 2001).

In most of the La Sierrita sections, there is an erosional surface at the top of the sand-siltstone deposit, with no sediments preserved above. However, in several sections, a 2–10 cm thick orange-stained and indurated limestone devoid of microfossils disconformably overlies the topmost layer of unit 3. Within the studied area, only in the Los dos Plebes section 1 have marls of the Paleocene Velasco Formation (*P. eugubina* zone P1a) been found above this orange limestone (Fig. 4c). A PGE anomaly (0.3 ng/g Ir) with a roughly chondritic pattern, and a sharp drop in $\delta^{13}C$ values just within this limestone further marks the K-T boundary, similar to the La Lajilla or El

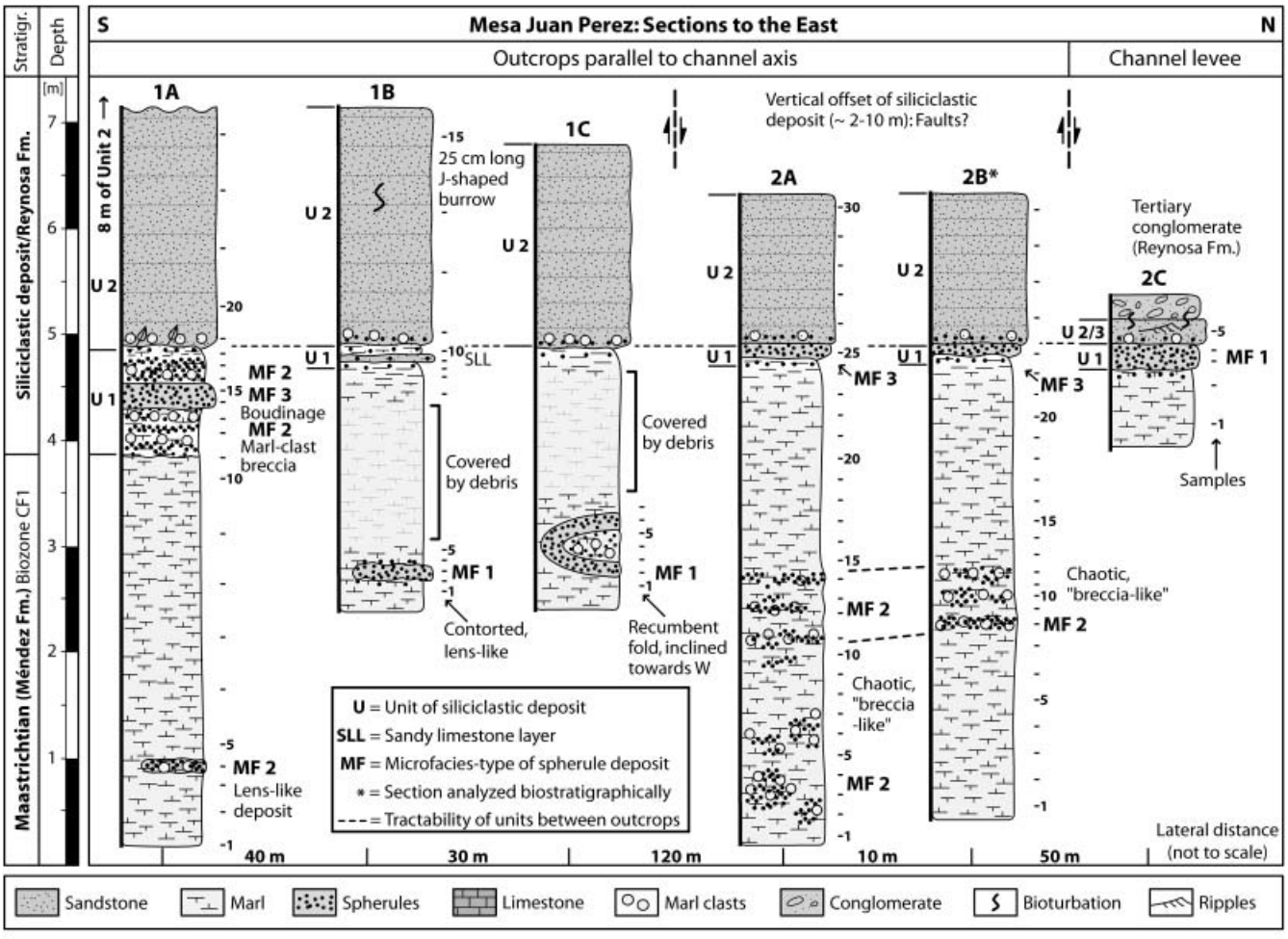


a

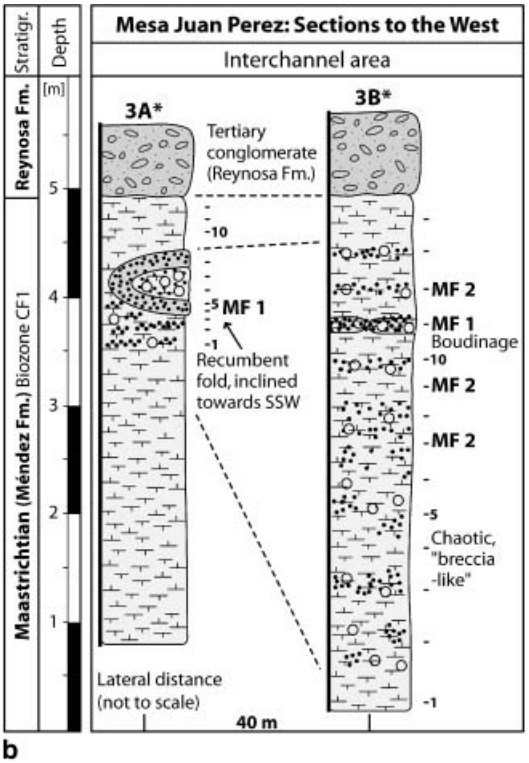


b

**Fig. 4a–c** Lithology and stratigraphy of sections with spherule deposits in the La Sierrita area. **a** and **b** Mesa Juan Perez, and **c** Maria de los Angeles and Los dos Plebes. The legend is provided in **a**. Note the lithologic variability and lateral discontinuity of spherule deposits embedded in marls of the late Maastrichtian (remember that the columns are not simply vertically directed, but inclined on the slope as shown in Fig. 2b). The large J-shaped burrow in the Mesa Juan Perez 1B section is interpreted as an escape burrow (Bromley 1996). The K-T boundary was found at the top of unit 3 of the sand-siltstone complex at the Los dos Plebes 1 section

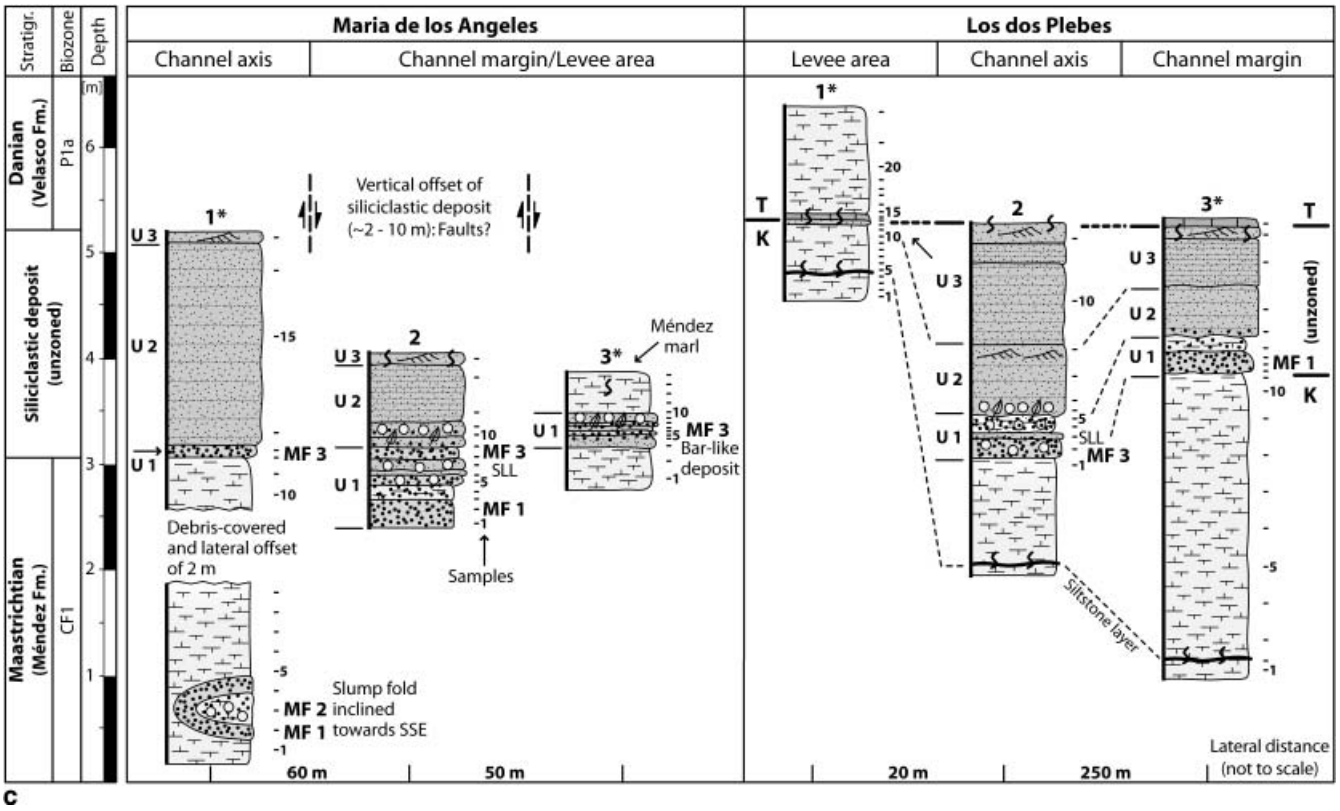


**Fig. 4c**

Mimbral section (Fig. 1; Smit et al. 1996; Lindenmaier et al. 1999).

## Stratigraphic and lithologic characteristics

### *Spherule-deposits interbedded in Méndez marls*

In the northern part of the La Sierrita area investigated for this study, sections with folded spherule deposits and chaotic marl-spherule mixtures interbedded in Méndez marls have been found in the Mesa Juan Perez and the Maria de los Angeles outcrop areas (Table 2, Fig. 2). The lateral extent, thickness, and lithology of spherule deposits are highly variable in these sections and, therefore, a description is provided for each location individually (Fig. 4).

The **Mesa Juan Perez sections 1A**, **1B**, **1C**, **2A**, and **2B** are located along the eastern flank of a prominent southward protrusion of the Mesa Juan Perez, 300 m northwest of the Rancho El Tecolote at longitude 99°31'053 and latitude 25°13'453 (Fig. 2). No spherule deposits within Méndez marls have been found along the opposite western flank of this protrusion, where eroded gullies expose Méndez marl below the sand-siltstone complex. The **Mesa Juan Perez section 1A** comprises a 30-cm-thick lens-like and marl clast-rich spherule deposit, embedded in Méndez marls, about 3 m below the sand-siltstone complex (Fig. 4a). Contacts to the under- and overlying Méndez marls are gradational and the lens-like spherule deposit is traceable over about 1 m laterally. In contrast, the spherule deposit at the base of the sand-siltstone complex can be traced about 10 m laterally and consists of a 20–30 cm thick indurated spherule layer that shows boudinage, pinches out to the northwest and is under- and overlain by 20–40 cm of marl-spherule mixtures with abundant flattened marl clasts (Fig. 3). This ‘marl clast-spherule breccia’ has sharp contacts to the indurated spherule horizon and the overlying sandstone of unit 2, as well as a gradational contact to the underlying Méndez marls. The **Mesa Juan Perez sections 1B** and **1C** contain a single, well-indurated 20–30 cm thick, lens-like spherule deposit that is traceable over several meters (Fig. 4a). Up to 2–3 m of Méndez marls, partly covered by debris on the slope, separate this spherule deposit from the spherule layer at the base of the sand-siltstone complex (unit 1). In these sections, the lower discontinuous spherule deposit is contorted, devoid of marl clasts, has sharp upper and lower contacts to the Méndez marls, and constitutes an overturned fold in the Mesa Juan Perez 1C section. This fold is inclined towards the west, with the direction of the fold axis at about 140–160°. Their core contains spherules and large rounded marl clasts. The upper (unit 1) spherule layer is 20–30-

**Table 2** Thickness of the spherule deposits and sand-siltstone units (see text for description) of the studied sections in the La Sierrita area; locations are shown in Fig. 2. Note that sections with spherule deposits embedded in Méndez marls have only been found in two outcrop areas, in contrast to the wider distribution of the unit 1 spherules layer. Abbreviations: w, strongly weathered; SLL, "sandy limestone layer"

| Section | Spherule deposit embedded in Méndez marl | Spherule deposit (Unit 1) | Unit 2 | Unit 3 |
|---|---|---|---|---|
| El Toro | – | 1.4 m, SLL | 4.1 m | 1.5 m |
| Los Cerritos | – | 0.3 m, SLL | 1.6 m | 0.3 m |
| Santa Rosa 1 | – | 0.1 m (w) | 1.8 m | 0.6 m |
| Nuevo Amanecer | – | 0.3 m, SLL | 1.1 m | 1.5 m |
| Mesa Juan Perez 1A | 0.2 m, lens-like | 1 m | 8 m | – |
| Mesa Juan Perez 1B | 0.2 m, lens-like, contorted | 0.3 m (w) | 2.5 m | – |
| Mesa Juan Perez 1C | 0.2 m, folded | 0.1 m (w) | 2.1 m | – |
| Mesa Juan Perez 2A | Breccia-like (~1.5 m) | 0.2 m | 1.2 m | – |
| Mesa Juan Perez 2B | Breccia-like (~1 m) | 0.2 m | 1.2 m | – |
| Mesa Juan Perez 2C | – | 0.3 m | – | 0.2 m |
| Mesa Juan Perez 3A | 0.3 m, folded | – | – | – |
| Mesa Juan Perez 3B | Breccia-like (up to 6 m) | – | – | – |
| Mesa Juan Perez 4A | – | 0.1 m (w) | 0.9 m | – |
| Mesa Juan Perez 4B | – | 0.3 m (w) | 2.4 m | – |
| El Tecolote | – | 0.2 m (w) | 3.1 m | 0.2 m |
| El Muerto | – | 0.3 m | 2.5 m | – |
| Maria de los Angeles 1 | 0.2 m, folded | 0.2 m | 1.9 m | 0.1 m |
| Maria de los Angeles 2 | – | 0.5 m SLL | 0.8 m | 0.1 m |
| Maria de los Angeles 3 | – | 0.4 m, SLL | – | – |
| Los dos Plebes 1 | – | – | – | 2 cm |
| Los dos Plebes 2 | – | 0.4 m, SLL | 1.4 m | 0.5 m |
| Los dos Plebes 3 | – | 0.3 m | 0.9 m | 0.2 m |

cm-thick, weathered with a friable matrix and contains a cm-thick sandy limestone. The lower contact with the Méndez marls is gradational and the upper contact with the overlying sandstone (unit 2) is abrupt. The **Mesa Juan Perez sections 2A** and **2B** contain scattered, 10–40-cm-thick, breccia-like marly spherule deposits, rich in rounded to angular marl clasts interbedded within Méndez marls (Fig. 3) and one 20-cm-thick, quartz-rich, and weathered spherule deposit at the base of the sand-siltstone complex (unit 1; Fig. 4a). The former have usually gradational transitions with the Méndez marls, whereas the latter has a sharp contact to the overlying sandstone (unit 2). Mesa Juan Perez 2B is equivalent to the Mesa Juan Perez 1 (JP) section described in Stinnesbeck et al. (2001). These scattered 'sedimentary breccias' extend over 2–4 m vertically.

The **Mesa Juan Perez sections 3A** and **3B** are located on a ridge-like southward projection of the Mesa Juan Perez, about 200 m from the main outcrop axis (Fig. 2b). In the **Mesa Juan Perez section 3A**, previously described by Soria et al. (2001, Figs. 1, 2), a 20–30 cm thick spherule deposit is present in a prominent 60-cm-thick fold within the Méndez marl (Figs. 3, 4b). The fold is inclined towards the SSE and the fold axis has a direction of about 80–90°. The core of the fold contains large rounded marl clasts, in part armored with spherules, and an indurated calcareous spherule layer with sharp upper and lower contacts. This particular spherule layer is exposed laterally over about 10 m. Isolated spherule-rich lenses are present in the marls below the fold. From this fold and along the steep slope, the spherule-rich layers grade laterally in irregular spherule-rich domains 'floating' in a reconstituted marl matrix that can be traced towards the east up to the **Mesa Juan Perez 3B section**, where these sedimentary marl-spherule breccias are patchily distributed along the slope over 4–6 m in the vertical and 10 m in the horizontal direction (Fig. 4b). Conglomerates of the Tertiary Reynosa Formation disconformably overlie the Méndez marls in both sections (Figs. 2, 3, 4b).

The **Maria de los Angeles section 1** is located on the southeastern flank of the hill, 400 m southeast of the Rancho El Tecolote at longitude 99°31'023 and latitude 25°14'003 (Fig. 2a). In this section, an indurated, 20–30 cm thick folded spherule deposit is present at the slope, extending about 2 m laterally (Fig. 4c). Three meters of Méndez marls partly covered by debris on the slope separate this spherule layer from the spherule layer at the base of the sand-siltstone complex (unit 1). The lower spherule deposit is devoid of marl clasts, has sharp upper and lower contacts to the Méndez marls, and constitutes an overturned fold inclined towards SSE, with the direction of the fold-axis about 70–90°. The core of the fold contains spherules and large rounded marl clasts that are armored by spherules. The upper (unit 1) spherule layer is 20–30 cm thick and indurated to highly weathered. The lower contact with the Méndez marls is gradational, whereas the upper contact with the overlying sandstone (unit 2) is abrupt.

### *Spherule deposits at the base of the sand-siltstone complex*

Outcrops with a spherule layer (unit 1) at the base of the sand-siltstone deposit are present in many locations in the

La Sierrita area (Table 2, Figs. 2, 4), as well as in numerous sections throughout northeastern Mexico (Fig. 1; Smit et al. 1992b, 1996; Stinnesbeck et al. 1993, 1996; Keller et al. 1994, 1997; Arz et al. 2001; Soria et al. 2001). In these outcrops, unit 1 varies with respect to thickness, composition, and degree of weathering. It is between 20 and 60 cm thick and consists of variably friable to indurated, alternating layers rich in either spherules, fragments, carbonate clasts, and sand, or spherule-marl mixtures, in addition to the presence of large round or flattened marl clasts (>25 cm in diameter) that may accumulate locally as 'marl clast breccias'. Occasionally, sandy limestone layers ("SLL" of Stinnesbeck et al. 1993; Keller et al. 1997) are interbedded. The indurated spherule- and sand-layers are structureless or slightly laminated, rarely graded, not bioturbated, frequently show boudinage, and may be tilted upwards with signs of lateral movement ('squeezing'). In some sections, the base of unit 1 constitutes a sharp, scoured surface on top of the Méndez marls, whereas in most sections the transition to the underlying Méndez marl is more gradational. The upper contact with the overlying sandstone (unit 2 or 3) is abrupt and at the base of this sandstone, horizons of interbedded spherules, plant fragments, and large marl clasts occur in addition to flute casts that indicate a current from the northwest during deposition. These current directions have been further confirmed by NW–SE trending gutter casts at the base of the El Toro and the Los dos Plebes 3 section.

## Petrographical, mineralogical and geochemical characteristics

### *Petrographic features of components*

Based on microscope examination of petrographic thin-sections, the main components of spherule deposits in the La Sierrita area are spherules, fragments (as defined below), carbonate clasts, marl clasts, and rare benthic foraminifera, in addition to a variable amount of siliciclastic detritus such as quartz and feldspar (Table 3, Figs. 5, 6). These components show no obvious morphological differences between different deposits and localities, and no size sorting or distinct abrasion features have been observed. Therefore, the following petrographic results apply to all spherule deposits analyzed in the area studied.

**Spherules and fragments** are present as the end members of a 'morphological mixing line' between 'spherules', which are generally round, elongate or teardrop- to dumbbell-shaped and 'fragments', which are irregularly shaped, in blocky or filamentous forms (Figs. 5, 6). The relative amount of spherules to fragments varies between 1:1 and 3:1 (Table 3). Occasionally, spherules and fragments are broken with fractures that cut through internal structures and cavities and some fragments have 'foam- or pumice-like' textures with stretched-out and attenuated films between other constituents. Some individuals present rims of coarse and radially aligned calcite crystals, resulting in a cauliflower-like appearance. Spherules and fragments exhibit intense green, brown-orange colors and ubiquitous opaque phases in plain light that may indicate the presence of chlorite, hematite, goethite, and palagonite, whereas translucent colors correspond to glassy spherules as revealed by electron microprobe analysis (see below).

Internal structures of spherules and fragments (Figs. 5, 6, 7, 8) include schlieren, vesicles, cracks, and irregular to globular inclusions of micrite, opaque or spar calcite phases. In addition, light-colored globular structures of round, elongate, or twisted shape are present. Schlieren exhibit a distinct flow-pattern, are light or opaque colored, and are often attenuated near embedded clasts. Spherules and fragments are generally devoid of microliths, but some are filled by small twinned crystals with swallow-tails and a typical criss-crossing texture, dark hair-like whiskers, or thin skeletal and branching crystals. Vesicles reach up to 75 % of the spherule volume and have smooth internal surfaces, exhibiting peeled 'onion-ring-like' opaque coatings that consist of tiny hematite or rutile crystals. They are filled with calcite, micrite, and zeolites. Most calcite infillings consist of coarse sparite and no concentrically zoned drusy mosaic-like spar or geopetal calcite mineralization was observed. Larger vesicles are embedded with smaller ones, thus resembling 'composite' spherules.

**Carbonate clasts** are a significant component of all spherule deposits in the La Sierrita area. Two categories can be distinguished (Figs. 5, 6): (1) angular carbonate clasts that are made of fine-grained calcite or coarse blocky spar calcite. These carbonate clasts may show circular inclusions of dark micrite or tiny randomly distributed opaque minerals. In addition, carbonate globules are suspended within spherules and fragments with a 'foam-/emulsion-like' texture. (2) Spherical or drop-shaped globules that consist of a single calcite crystal or of thin, sometimes curved, and elongate needle-like calcite crystals ('feathery texture') that are radially arranged around small inclusions and show outward skeletal branching. These outward-radiating calcite crystals may form thick coatings on spherules, fragments, or marl clasts.

### *Microfacies analysis*

Based on thin section analysis of spherule deposits in the La Sierrita area, three types of microfacies can be recognized in the various deposits and locations as depicted in Fig. 4, though gradual transitions between these microfacies exist locally.

The **microfacies type 1** has been observed in the slump folds and at the base of the sand-siltstone complex in the channel margin area (Fig. 4). Commonly, microfacies type 1 is characterized by a dense, chaotic, grain-supported texture, resembling a sedimentary polymict microbreccia (Fig. 5a, b), though sometimes constituents

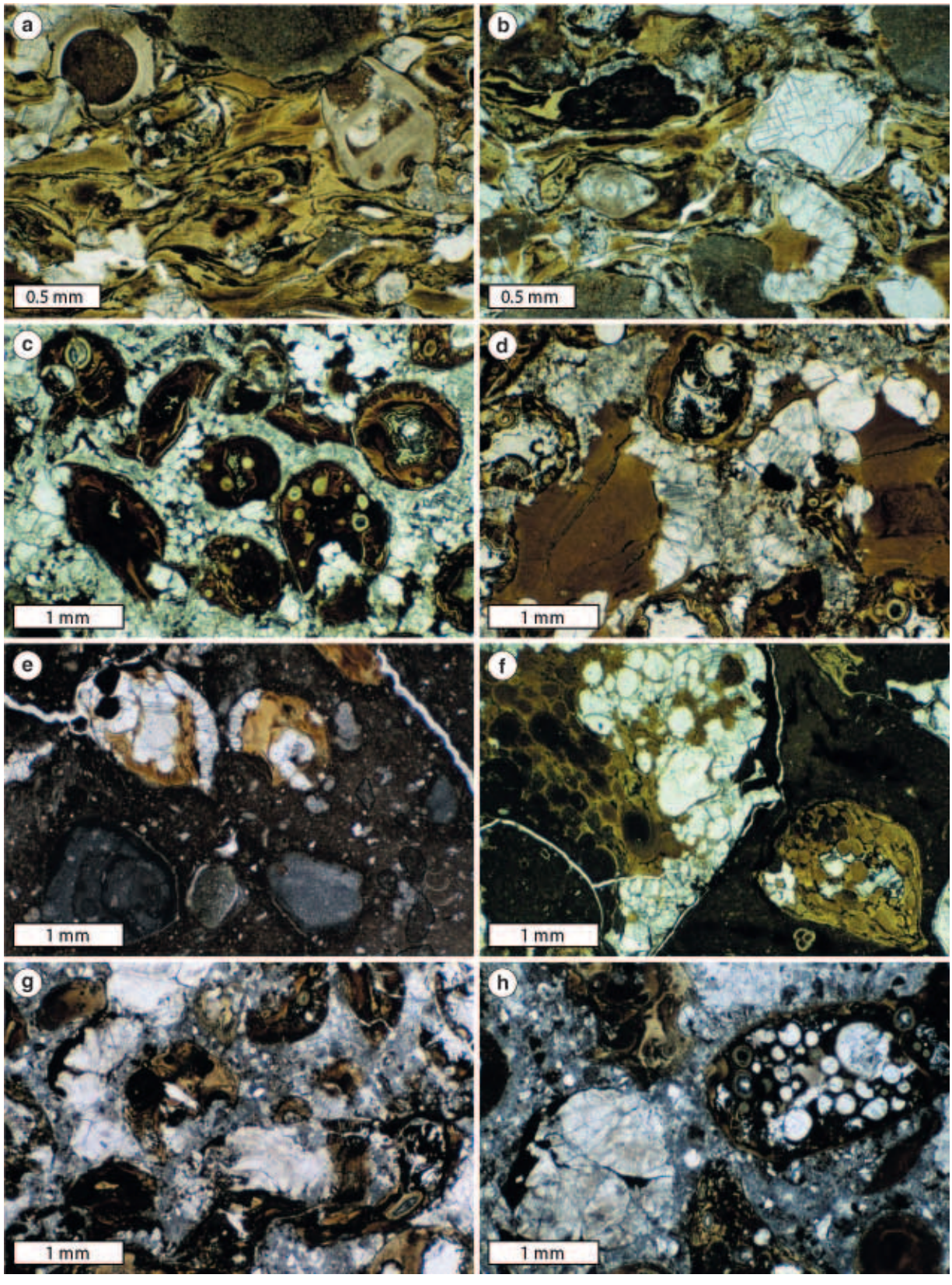


**Fig. 5a–h** Thin section microphotographs of spherule deposits in the La Sierrita area (plane polarized light), showing the three types of microfacies distinguished. **a–d** Microfacies type 1 with microbreccia-like texture, high interstitial pore space, and vesiculated spherules that are in part welded (concave-convex contacts), or broken. Note the random orientation of grains and presence of fragments with characteristic flow patterns that enclose spherules, carbonate clasts, marl clasts, and benthic foraminifera. **e–f** Microfacies type 2 is characterized by spherules, fragments, and marl clasts 'floating' in a marl matrix. **g–h** Microfacies type 3 with spherules, fragments, carbonate, clasts, and minor terrigeneous debris (e.g., quartz, feldspar), revealing bimodal grain-size distribution and rarely preferred dimensional orientation of grains. Note presence of delicately shaped spherules and fragments

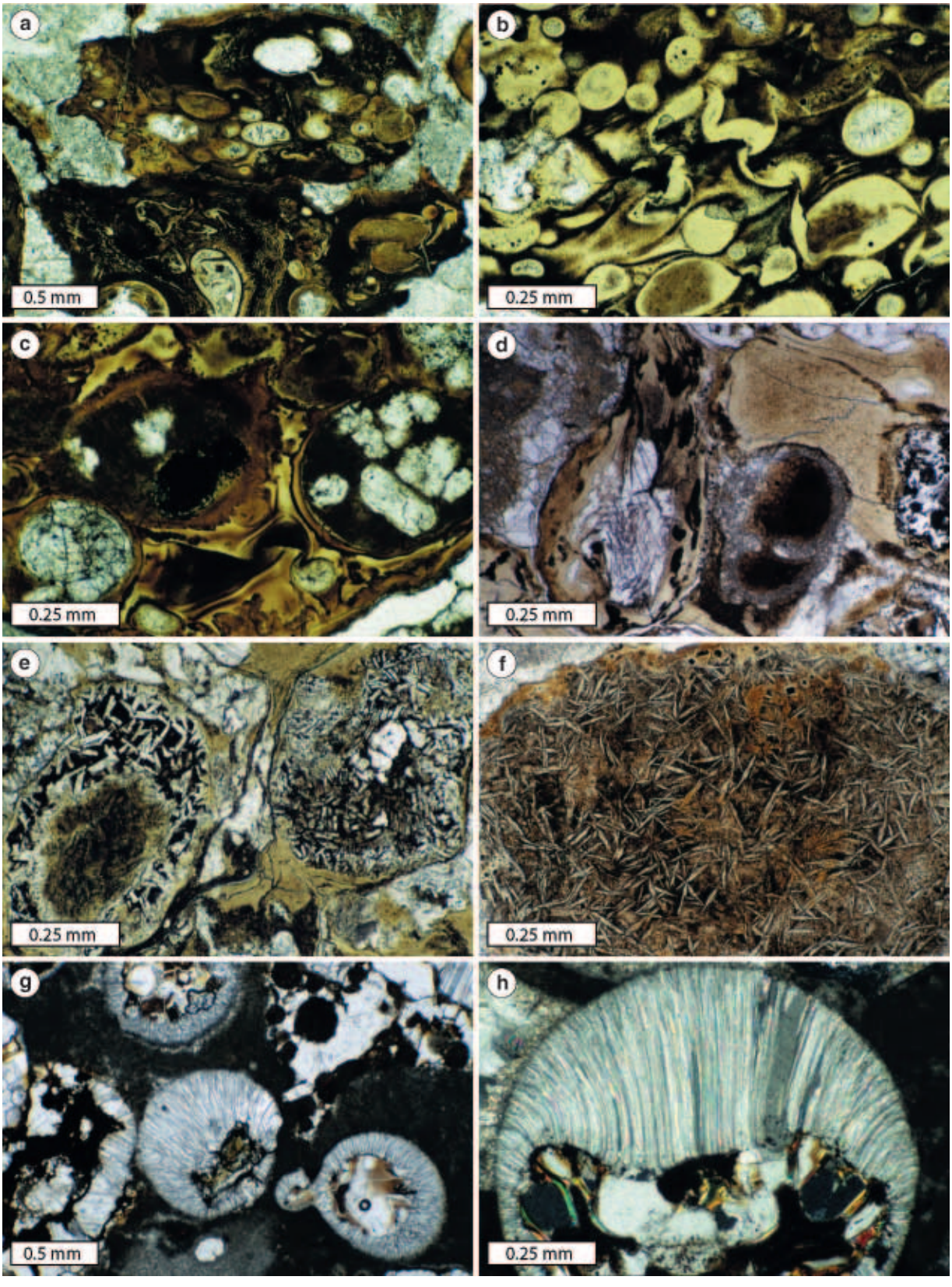


**Fig. 6a–h** Thin section microphotographs of spherule deposits in the La Sierrita area, showing characteristic features of components in plane polarized light. **a** Two attached spherules with related internal deformation of vesicles, schlieren, and various globules that indicate flow pattern and deformation structures. Vesicles are filled by calcite, clay minerals, or silicic phases (tridymite?). **b** Spherule attached to a fragment that encloses a thick-walled benthic foraminifera. **c** and **d** Details of internal spherule structures with schlieren, dark micritic inclusions, and carbonate inclusions. **e** Euhedral feldspar-like microliths (in part twinned) in spherule, pseudomorphically displaced by calcite. **f** Euhedral branched skeletal microliths, presumably quenched olivine, or pyroxene. **g** Emulsion-like textures in spherules filled by calcite, silicic phases and micrite; note the upper left edge of broken spherule, which indicates that these features are not of diagenetic origin. **h** Spherule fragment rimmed by radially orientated, bent, and needle-like calcite crystals (crossed nicols)

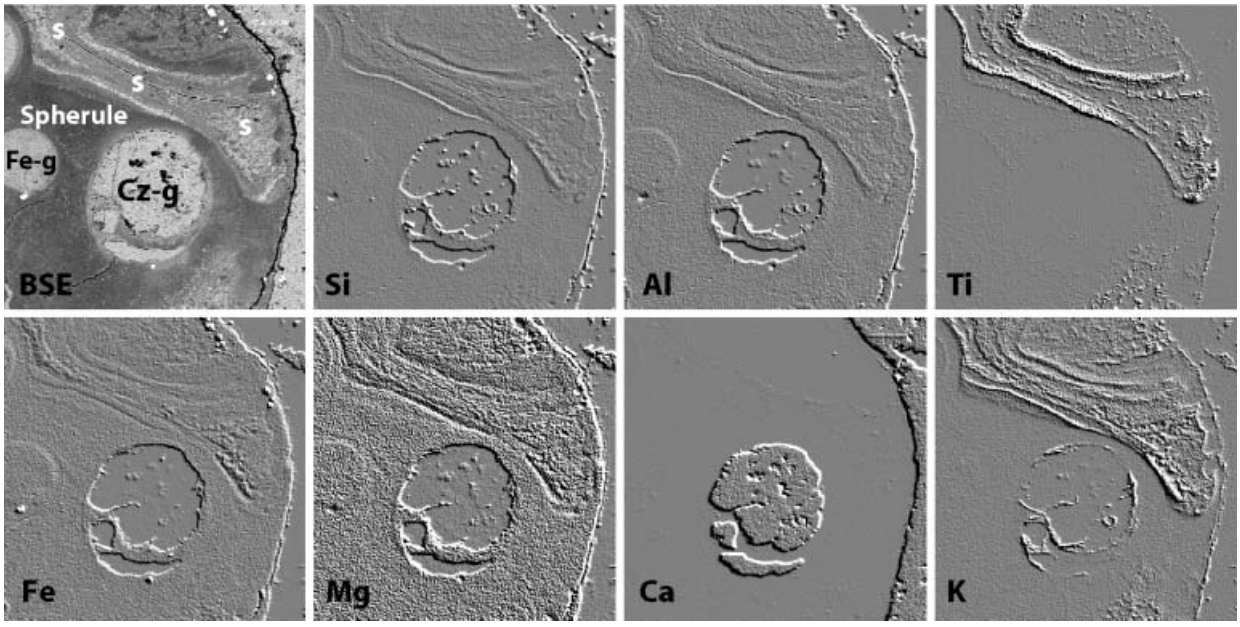


**Fig. 7** BSE image and artificially illuminated qualitative element distribution maps of a spherule from the Mesa Juan Perez section 1B (sample 3). Length of each field is 0.5 mm. High relief indicates high concentrations (illumination from the *upper right*). These maps show the Fe-, Al-, and Mg-rich spherule composition with K-, Ti-rich schlieren (*s*) and calcite globules/vesicles? (*Cz-g*). In addition, small globules enriched in Fe and Mg (*Fe-g*) are present and crystals of hematite (*h*) line the spherule rim

**Table 3** Modal composition of spherule deposits in the La Sierrita area as determined by petrographic analysis (see text). Data are given as vol%. Note the large variability of composition, but the similarity in ranges of all three microfacies-types observed

| Microfacies-type | Spherules | Fragments | Carbonate clasts | Detritus (Qtz/Fdsp) | Marl clasts | Mean diameter of spherules (mm) |
|---|---|---|---|---|---|---|
| (1) 'Microbreccia-like' | 30–70 | 10–30 | 15–40 | <5 | Rare–common | ~0.8 |
| (2) 'Marly' | 25–35 | 10–20 | 20–40 | <5 | Frequent[a] | ~1 |
| (3) 'Detritus-enriched' | 30–60 | 10–20 | 5–20 | 5–25 | Rare[a] | ~0.8 |

are loosely 'floating' in a gray matrix of sparitic calcite. Constituents include spherules, fragments, carbonate clast, marl clasts, and occasional benthic foraminifera; their relative amounts are shown in Table 3. In this microfacies, many spherules and fragments appear welded together and large clusters are present with concave-convex contacts and concomitant deformation of internal structures. In addition, spherules and fragments, as well as marl clasts appear to have been reshaped plastically along their contacts and frequently enclose each other, thus giving an 'amalgamated' appearance to this microfacies. Thin sections cut at various angles to the bedding reveal that these welded and amalgamated constituents build up three-dimensional mesh-/foam-like structures. Locally, microfacies type 1 shows a distinct spherule-enrichment (up to 70 vol%), resulting in a relative depletion of fragments and carbonate clasts (Fig. 5c, d). In microfacies type 1, no terrigeneous detritus was observed. The grain sizes of spherules range from 0.4–10 mm, with a mean diameter of about 0.8 mm, and the grain sizes of fragments and carbonate clasts range from 0.5–10 mm. In this microfacies, planktonic and benthic foraminifera are rare, though the genera *Anomalina*, *Cibicidoides*, *Lenticulina*, *Neoflabellina*, *Tritaxia*, and *Palmula* have been identified (R. Speijer, personal communication 2000).

The **microfacies type 2** was found in marl-spherule mixtures within Méndez marls and at the base of the sand-siltstone complex in the channel axis area (Fig. 4). It is distinguished from type 1 by its micritic (marly) matrix and a mud-supported texture, thus revealing a variable mixture with Méndez marls (Fig. 5e, f). In contrast to microfacies 1, welding and amalgamation of constituents are rarely observed. This microfacies type shows no PDO fabric and components are loosely floating in the matrix. The main constituents of microfacies 2 and their relative abundances are similar to microfacies 1 (Table 3). Terrestrial detritus is present only in the fine fraction (<63 μm) of the marl matrix. Spherules and fragments range between 0.3 and 8 mm in size, with a mean diameter of about 1 mm. In this microfacies type, predominantly upper Cretaceous planktic foraminifera (mainly Pseudotextularidae and Globotruncanidae) have been found, whereas benthic foraminifera are rare and no identifiable individuals have been detected.

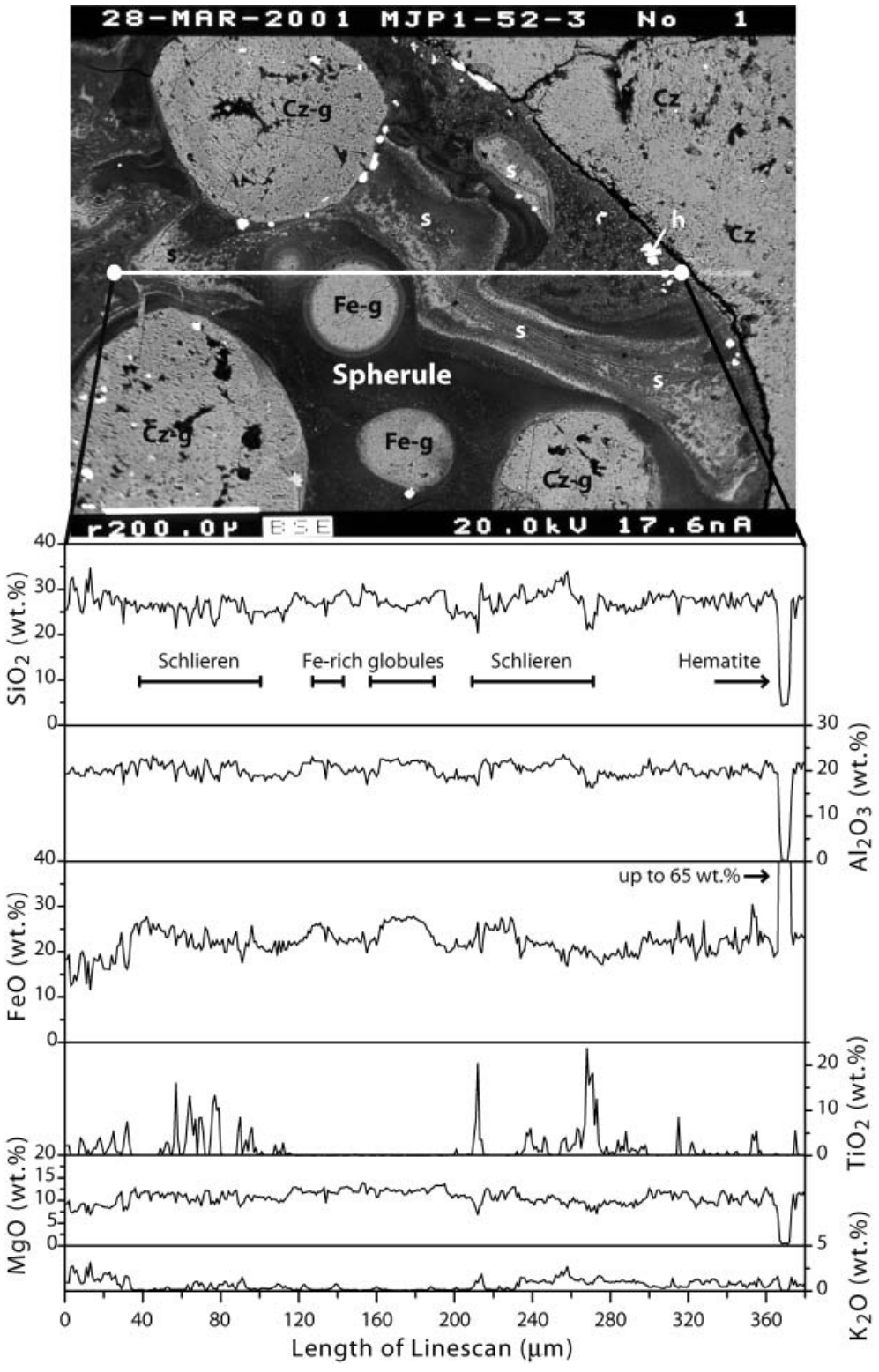


**Fig. 8** BSE image and quantitative electron microprobe traverse across the spherule that is depicted in Fig. 7. Abbreviations are given in Fig. 7

The **microfacies type 3** was observed at the base of the sand-siltstone complex in the channel axis to margin area (Fig. 4). It shows a grain-supported texture with a micrite matrix; a preferential orientation of the grains is rarely developed (Fig. 5g, h). This microfacies consists of spherules, fragments, and carbonate clasts, in addition to a variable amount of detritus (5–25 %) such as quartz and feldspar (Table 3). Rounded marl clasts are present as minor components. Similar to microfacies 2, welding and amalgamation of constituents are rarely present. Quartz and feldspar range between 0.03 and 0.1 mm in diameter, with a mean of about 0.1 mm, and spherules range

**Table 4** XRD analysis of the bulk rock mineralogy (in counts) and the semi-quantitative clay mineralogy of the insoluble residue (in rel % of the <2 μm fraction) from spherule deposits in the La Sierrita area. Results are grouped according to their microfacies-types

| XRD | Sample[a] | Quartz Counts | Feldspar Counts | Calcite Counts | Smectite Counts | Chlorite[b] Rel % | Illite Rel % | Illite-smectite Rel % | Rel % |
|---|---|---|---|---|---|---|---|---|---|
| Microfacies 1 | MJP1B-3 | 96 | 34 | 7695 | 2 | 77 | 14 | 6 | |
| | MAS1-2 | 61 | 18 | 8677 | <2 | 100 | <2 | <2 | |
| | MAS2-2 | 80 | 12 | 6487 | <2 | 59 | 32 | 9 | |
| | LPD3-14 | 152 | 16 | 5046 | <2 | 95 | 5 | <2 | |
| | MJP1C-2 | 162 | 25 | 5830 | 2 | 95 | 3 | <2 | |
| | MJP3A-4 | 59 | 14 | 2587 | <2 | 98 | 2 | <2 | |
| Microfacies 2 | MJP2B-8 | 649 | 128 | 1404 | <2 | 64 | 27 | 9 | |
| | MJP2B-10 | 869 | 148 | 4592 | 1 | 46 | 38 | 16 | |
| | MJP2B-12 | 965 | 221 | 1937 | 2 | 55 | 37 | 6 | |
| Microfacies 3 | MJP2B-23 | 815 | 309 | 617 | 2 | 53 | 27 | 17 | |
| | MAS1-14 | 463 | 277 | 5420 | 7 | 87 | 6 | <2 | |
| | LPD2-2 | 515 | 21 | 4328 | <2 | 39 | 33 | 32 | |
| | SRS-1 | 151 | 110 | 4533 | 20 | 36 | 28 | 24 | |
| | SRS-2 | 527 | 43 | 5871 | 3 | 88 | 10 | <2 | |
| | MJP1A-14 | 231 | 147 | 2148 | 4 | 83 | 4 | 9 | |
| | MJP1A-15 | 225 | 85 | 4339 | 3 | 89 | 5 | 3 | |
| Méndez marl | (*n*=19) | 2775 | 215 | 2240 | 6 | 39 | 41 | 13 | |
| | SD | 912 | 45 | 419 | 4 | 8 | 13 | 5 | |

[a] Abbreviations are as follows: MJP, Mesa Juan Perez; MAS, Maria de los Angeles; LDP, Los dos Plebes; SRS, Santa Rosa Sur; SD, standard deviation

[b] Including chlorite-smectite mixed layers with <5–10% smectite

**Table 5** WDS and EDS data of major and trace elements from bulk rock spherule deposits of the La Sierrita area. Values are given in wt% for the major elements, in ppm for trace elements, total Fe is reported as $Fe_2O_3$, LOI is loss of ignition. Abbreviations are given in Table 3

| WDS | Sample | $SiO_2$ | $TiO_2$ | $Al_2O_3$ | $Fe_2O_3$ | MnO | MgO | CaO | $Na_2O$ | $K_2O$ | $P_2O_5$ | LOI |
|---|---|---|---|---|---|---|---|---|---|---|---|---|
| Microfacies 1 | MJP1B-3 | 16.79 | 0.55 | 10.32 | 12.31 | 0.09 | 5.61 | 27.76 | 0.06 | 0.34 | 0.12 | 26.35 |
| | MAS1-2 | 9.41 | 0.27 | 5.95 | 7.89 | 0.09 | 3.74 | 37.16 | 0.03 | 0.11 | 0.08 | 34.06 |
| | MAS2-2 | 14.34 | 0.38 | 9.08 | 10.62 | 0.07 | 4.51 | 26.45 | 0.05 | 0.38 | 0.11 | 29.68 |
| | LDP3-14 | 15.24 | 0.35 | 9.03 | 9.46 | 0.11 | 4.17 | 33.62 | 0.08 | 0.61 | 0.10 | 27.00 |
| Microfacies 2 | MJP2B-8 | 28.79 | 0.52 | 10.80 | 8.00 | 0.06 | 3.95 | 19.13 | 0.58 | 1.31 | 0.11 | 27.39 |
| | MJP2B-12 | 25.23 | 0.40 | 7.98 | 4.47 | 0.05 | 2.60 | 16.56 | 0.54 | 1.31 | 0.10 | 21.14 |
| | MJP2B-10 | 34.70 | 0.47 | 10.78 | 5.29 | 0.08 | 3.30 | 23.92 | 0.82 | 1.81 | 0.14 | 21.79 |
| Microfacies 3 | MJP2B-23 | 38.52 | 0.99 | 14.82 | 14.48 | 0.05 | 4.09 | 8.02 | 0.76 | 0.68 | 0.15 | 12.12 |
| | MAS1-14 | 22.60 | 0.34 | 8.50 | 8.99 | 0.12 | 3.63 | 31.24 | 0.49 | 0.37 | 0.14 | 27.00 |
| | LDP2-2 | 15.16 | 0.35 | 6.55 | 6.74 | 0.13 | 2.08 | 35.74 | 0.15 | 0.41 | 0.07 | 32.38 |
| | SRS-1 | 16.38 | 0.33 | 7.78 | 7.10 | 0.11 | 2.89 | 31.81 | 0.19 | 0.75 | 0.07 | 30.00 |
| | SRS-2 | 22.32 | 0.27 | 8.20 | 8.38 | 0.08 | 3.47 | 28.56 | 0.57 | 0.39 | 0.11 | 26.33 |
| Méndez marl | *n*=40 | 43.71 | 0.47 | 11.51 | 4.49 | 0.02 | 1.88 | 19.57 | 0.87 | 2.03 | 0.13 | 15.15 |
| | SD | 2.07 | 0.03 | 0.64 | 0.24 | 0.01 | 0.11 | 1.89 | 0.09 | 0.14 | 0.02 | 1.46 |
| Sandstone | *n*=6 | 48.25 | 0.39 | 9.54 | 2.84 | 0.03 | 1.26 | 19.64 | 2.44 | 1.20 | 0.14 | 16.01 |
| (unit 2) | SD | 4.52 | 0.09 | 1.73 | 1.11 | 0.01 | 0.42 | 4.41 | 0.29 | 0.40 | 0.08 | 2.81 |

| EDS | Sample | Cu | Zn | Rb | Sr | Y | Zr | Ba | La | Ce |
|---|---|---|---|---|---|---|---|---|---|---|
| Microfacies 1 | MJP1B-3 | 26 | 58 | 10 | 550 | 10 | 72 | 320 | 10 | 30 |
| | MAS1-2 | 21 | 71 | 3 | 580 | 10 | 47 | 160 | 19 | 25 |
| | MAS2-2 | 16 | 58 | 18 | 470 | 15 | 48 | 2510 | <10 | <10 |
| | LDP3-14 | 17 | 63 | 13 | 500 | 17 | 63 | 6030 | <10 | <10 |
| Microfacies 2 | MJP2B-8 | 21 | 78 | 51 | 390 | 16 | 92 | 370 | 10 | 26 |
| | MJP2B-12 | 19 | 76 | 61 | 420 | 14 | 78 | 210 | 22 | 23 |
| | MJP2B-10 | 22 | 83 | 60 | 430 | 16 | 82 | 220 | 18 | 38 |
| Microfacies 3 | MJP2B-23 | 31 | 78 | 23 | 230 | 19 | 145 | 660 | 11 | 38 |
| | MAS1-14 | 17 | 53 | 10 | 410 | 15 | 72 | 400 | 10 | 27 |
| | LDP2-2 | 22 | 50 | 12 | 430 | 12 | 30 | 1760 | 14 | 26 |
| | SRS-1 | 24 | 81 | 23 | 620 | 15 | 58 | 4030 | <10 | <10 |
| | SRS-2 | 11 | 50 | 10 | 480 | 15 | 71 | 4560 | <10 | <10 |
| Méndez marl | *n*=40 | 20 | 84 | 76 | 390 | 15 | 91 | 500 | 42 | 90 |
| | SD | 4 | 16 | 9 | 70 | 2 | 10 | 50 | 13 | 19 |
| Sandstone | *n*=6 | 13 | 27 | 16 | 480 | 12 | 87 | 160 | 10 | 20 |
| (unit 2) | SD | 3 | 6 | 8 | 80 | 2 | 15 | 80 | 3 | 5 |
| Detection limit | | 5 | 4 | 10 | 1 | 3 | 5 | 5 | 10 | 10 |

**Table 6** Major element composition of spherules and fragments from the La Sierrita area by EMP analysis. About 4 to 8 individuals were measured in one sample. All values are in wt%, *n* corresponds to the number of analyses, *n.m.*, not measured, and total Fe is reported as FeO, additional abbreviations are given in Table 3

| La Sierrita | | $SiO_2$ | $TiO_2$ | $Al_2O_3$ | FeO | NiO | MgO | CaO | $Na_2O$ | $K_2O$ | Total |
|---|---|---|---|---|---|---|---|---|---|---|---|
| Iron-rich spherules and fragments (samples comprising microfacies 1) | | | | | | | | | | | |
| MJP1B-3 | avg. | 27.44 | 0.25 | 20.99 | 23.69 | n.m. | 11.80 | 0.55 | 0.05 | 0.31 | 85.09 |
| *n*=55 | SD | 1.62 | 0.52 | 1.16 | 1.87 | n.m. | 0.85 | 0.20 | 0.03 | 0.34 | 2.79 |
| MAS2-2 | avg. | 25.37 | 0.09 | 20.37 | 24.82 | n.m. | 10.49 | 0.36 | 0.04 | 0.16 | 81.69 |
| *n*=12 | SD | 0.79 | 0.08 | 0.86 | 1.44 | n.m. | 0.41 | 0.09 | 0.04 | 0.13 | 2.85 |
| LDP3-14 | avg. | 26.27 | 0.35 | 20.96 | 25.45 | n.m. | 11.28 | 0.43 | 0.02 | 0.09 | 84.86 |
| *n*=10 | SD | 1.09 | 0.44 | 1.42 | 2.25 | n.m. | 0.54 | 0.23 | 0.01 | 0.09 | 3.59 |
| Iron-rich spherules and fragments (samples comprising microfacies 3) | | | | | | | | | | | |
| MJP1A-14 | avg. | 27.21 | 0.21 | 21.71 | 24.28 | n.m. | 10.95 | 0.44 | 0.05 | 0.50 | 85.34 |
| *n*=44 | SD | 2.65 | 0.34 | 1.34 | 3.01 | n.m. | 0.95 | 0.62 | 0.07 | 0.54 | 3.66 |
| MJP1A-15 | avg. | 28.47 | 0.10 | 22.47 | 24.09 | n.m. | 10.73 | 0.61 | 0.04 | 0.53 | 87.10 |
| *n*=75 | SD | 2.55 | 0.43 | 1.17 | 2.12 | n.m. | 0.93 | 0.20 | 0.03 | 0.60 | 2.72 |
| MAS1-14 | avg. | 28.80 | 0.34 | 22.29 | 25.80 | n.m. | 9.65 | 0.79 | 0.03 | 0.46 | 88.17 |
| *n*=20 | SD | 1.65 | 0.59 | 0.77 | 1.18 | n.m. | 0.52 | 0.14 | 0.01 | 0.39 | 1.47 |
| K-rich glass spherules and fragments (samples comprising microfacies 1 and 3) | | | | | | | | | | | |
| LDP3-14 | avg. | 50.23 | 0.19 | 29.15 | 1.88 | n.m. | 2.35 | 0.57 | 0.10 | 7.25 | 91.79 |
| *n*=21 | SD | 1.16 | 0.13 | 0.78 | 0.54 | n.m. | 0.29 | 0.07 | 0.04 | 0.21 | 1.20 |
| SRS-2 | avg. | 50.12 | 0.15 | 29.55 | 1.49 | n.m. | 2.14 | 0.56 | 0.10 | 7.14 | 91.30 |
| *n*=12 | SD | 0.62 | 0.10 | 0.46 | 0.09 | n.m. | 0.07 | 0.05 | 0.04 | 0.19 | 1.05 |
| Schlieren in spherules and fragments (representative single points) | | | | | | | | | | | |
| MJP1A-14 | | 33.33 | 4.54 | 23.47 | 19.07 | n.m. | 7.59 | 0.59 | 0.02 | 2.55 | 91.15 |
| MJP1B-3 | | 30.79 | 3.44 | 23.43 | 20.60 | n.m. | 9.56 | 0.36 | 0.11 | 1.76 | 90.05 |
| MAS2-2 | | 18.21 | 14.04 | 17.94 | 28.66 | n.m. | 7.07 | 1.09 | 0.08 | 0.24 | 87.39 |
| Hexagonal and octahedral inclusions in spherules and fragments (representative single points) | | | | | | | | | | | |
| MJP1A-14 | | 3.82 | 0.05 | 0.09 | 72.44 | 0.32 | 0.39 | 1.61 | 0.02 | 0.02 | 78.83 |
| MJP1C-2 | | 3.77 | 0.1 | 0.63 | 71.09 | 0.37 | 0.59 | 0.42 | 0.09 | 0.02 | 77.2 |
| MAS2-2 | | 4.23 | 0.05 | 0.48 | 71.82 | 0.31 | 0.56 | 0.57 | 0.04 | 0.03 | 78.09 |

between 0.3 and 10 mm in diameter, with a mean of about 0.8 mm. Grain-size distribution is, thus, strongly bimodal. Planktonic or benthic foraminifera are rare in this microfacies and no identifiable genera have been detected.

*Mineralogical phases*

The results of the XRD analysis for the bulk rock and the clay-size fraction of spherule deposits and Méndez marls are shown in Table 4. Bulk rock analysis revealed high amounts of calcite and minor amounts of quartz and feldspar. In addition, trace amounts of gypsum, ankerite, hematite, goethite, and dolomite are present. The three microfacies types can be well distinguished, with the microfacies types 1 and 3 revealing strong similarities and only minor detrital influx, whereas the Méndez marl admixed in microfacies 2 is reflected by increased quartz and feldspar and less abundant calcite. Analysis of oriented and glycolated samples identify the predominant clay minerals as trioctahedral Fe- and Mg-rich chlorites and chlorite-smectite mixed layers (<10 %) characterized by a low content of expandable layers (~5–10 % smectite; Bailey 1988; Moore and Reynolds 1997). These chlorites comprise about 40–90 % of the <2 μm fraction. In addition, low amounts of illite-smectite mixed layers and mica are present; occasionally, higher amounts (up to 30 %) of these clay minerals reflect increased admixture of Méndez marls. Smectite is well below 5 %. The admixed Méndez marl within microfacies type 2 is reflected by less abundant chlorite and by a significant increase of mica.

*Geochemical composition*

**Bulk-rock WDS- and EDS-analyses** are shown in Table 5. The results for the elements Cr, Ni, As, and Pb, measured by EDS, are below or near the detection limit (Cr, Ni: 50 ppm; As, Pb: 5 ppm), and are therefore not listed in Table 5. The microfacies type 1 spherule deposits have variable major element contents with CaO contents of 25–40 wt%, in addition to $SiO_2$, FeO, $Al_2O_3$ (~5–15 wt% each), and minor MgO (~5 wt%). $TiO_2$, $K_2O$, MnO, $Na_2O$, and $P_2O_5$ are below 1 wt%. Trace elements show relatively uniform values; only the Ba contents are widely scattered. Microfacies type 2 spherule deposits differ from microfacies type 1 by higher $SiO_2$, $K_2O$, and $Na_2O$ contents, whereas the CaO, FeO, and MgO contents are significantly lower. They also show higher Rb contents, slightly elevated Zr contents, and a more limited range of Ba concentrations. This composition reflects the mixing with Méndez marl as also revealed by the

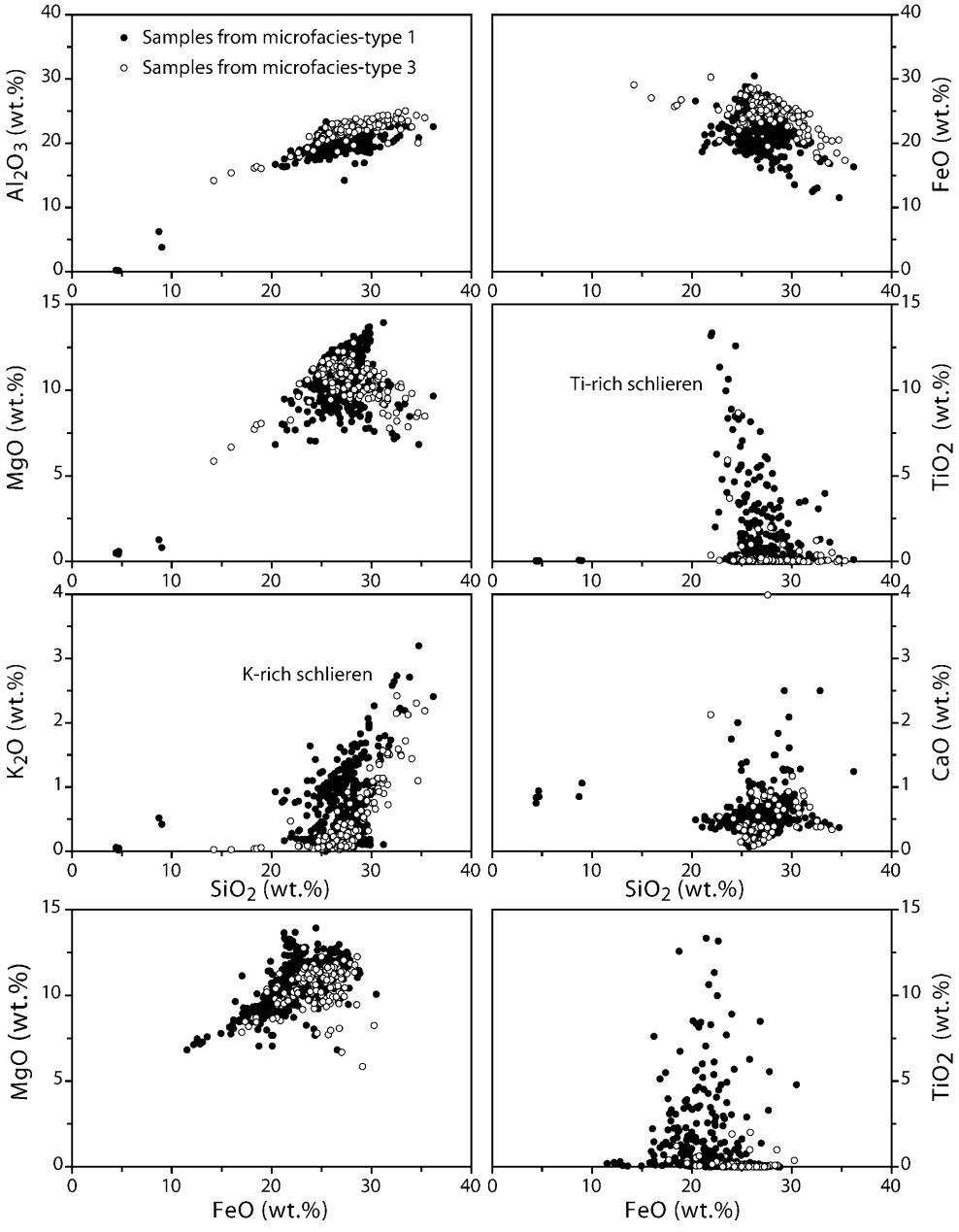


**Fig. 9** Oxide correlation diagrams of spherules and fragments from the La Sierrita area with results from all individual microprobe analyses (except for the K-rich mafic glass spherules) that are summarized in Table 6 and from the linescan that is shown in Fig. 8. Note that results from spherule deposits comprising microfacies type 1 (*filled circles*) are within the same range as results from microfacies type 3 spherule-deposits (*open circles*)

petrological and mineralogical analysis. In terms of major elements, microfacies type 3 spherule deposits show variable CaO, $SiO_2$, and FeO contents that are similar to microfacies 1; this similarity exists also in terms of the trace element composition.

**Electron microprobe analyses:** the results from single point, linescan, and area measurements are shown in Table 6 and Figs. 7, 8, and 9. Spherules and fragments comprise two distinct compositional phases: (1) a prevalent FeO- (25–35 wt%), $Al_2O_3$- (17–22 wt%), MgO- (10–15 wt%) rich phase with about 20–25 wt% $SiO_2$ and low alkali content (>1 wt%), that exhibits low total oxides of 80–90 wt%, thus indicating strong hydration. This composition corresponds to chlorite; according to Newman and Brown (1987), chlorites are placed in between the Fe- and Mg-rich end members of the chlorite group (chamosites and clinochlores). Analyses from various spherules and fragments within one sample or samples from different microfacies types show no relevant differences (Table 6, Fig. 9). (2) A rare K-rich mafic glass phase ($SiO_2$ 45–50 wt%, $Al_2O_3$ 25–30 wt%, $K_2O$ 5–8 wt%) with low Fe and Mg contents (<2–3 wt%). These K-rich mafic glass spherules and fragments show total oxides of 90–95 wt%, thus indicating slight hydration.

Within spherules and fragments, several textural domains show a markedly different composition (Table 6, Figs. 7, 8, 9, 10): (1) Schlieren that are enriched either in FeO, $TiO_2$ or $K_2O$. (2) Globules (sometimes distorted) that are slightly enriched in FeO and MgO, and depleted in $SiO_2$. (3) Hexagonal and octahedral inclusions, about

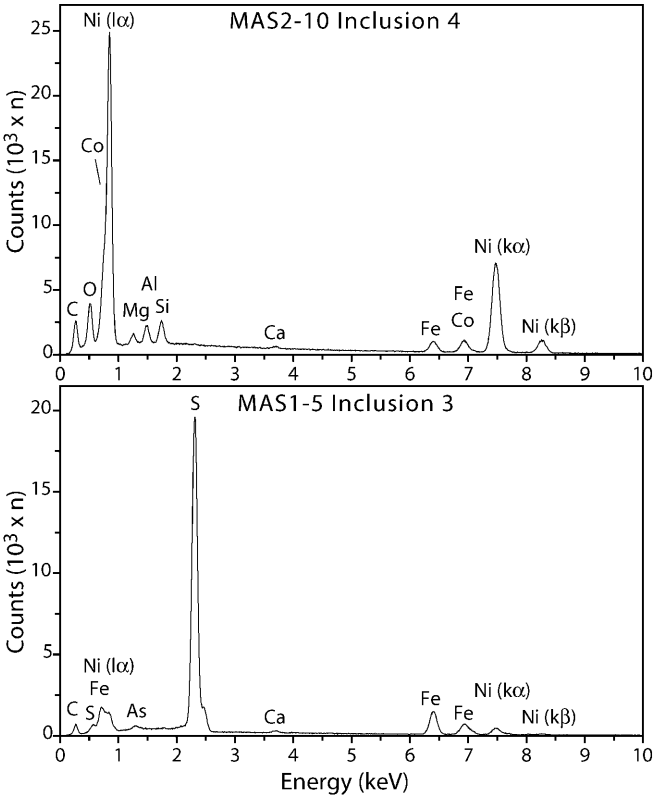


**Fig. 10a, b** EDS spectra of **A** 'metallic' and **B** 'sulfidic' Ni-, Co-rich inclusions in spherules and carbonates from La Sierrita (with 15 keV acceleration voltage). The weak Mg, Al, Si, and Fe peaks in **a** and Ca peaks in **b** derived from the enclosing spherule and carbonate, respectively

10–20 μm in diameter that comprise hematite, rutile, and Ti-Fe oxides. These inclusions may be arranged in a wreath-like fashion. Frequently, hematite crystals are slightly enriched in $SiO_2$ and in NiO. Ti-Fe oxides may show a dendritic or skeletal appearance, or present garland-shaped lamellae with crystal sizes of the oxides growing towards the interior of grains. (4) Rare μm-sized globular or irregular inclusions of either Fe-, Ni-, Co-rich metallic or Ni-rich sulfide composition.

## Interpretation and discussion

### Origin of spherule deposits

Spherule deposits from the La Sierrita area are texturally and compositionally complex and exhibit various petrologic features and geochemical ranges that allow for an evaluation of their origin and comparison with spherule deposits in other K-T boundary localities.

#### *Implications from petrological characteristics*

**Spherules and fragments:** the characteristic morphological features of spherules, including their fluidal-shaped forms and internal textures, such as vesicles and schlieren are indicative of an origin as molten droplets from a highly fluid melt with subsequent exsolution of a gas phase due to pressure release and cooling (Shelley 1993; Engelhardt et al. 1995). The same applies to the angular fragments with similar flow textures, though their irregular shapes and less abundant vesicles point to a different thermal history and indicate either fragmentation in a ductile-rigid state by turbulence in the air, or by thermal stress due to quenching with water (Glass et al. 1997). Pyroclasts of comparable size and shape have been described for impact ejecta (Stähle 1972; Graup 1981; Glass 1990; Izett 1991; Engelhardt et al. 1995; Dressler and Reimold 2001), as well as for specific volcanic processes (Cas and Wright 1987; Fisher and Schmincke 1984; Robin et al. 1996). However, a volcanic origin seems unlikely, as the coarse grain size of the La Sierrita spherule deposits would require a nearby vent (Fisher and Schmincke 1984) and to date no volcanic source is known close to La Sierrita (e.g., Perez Cruz 1993). Thin fine-grained ash beds are sometimes present in the Méndez marl, but these contain no spherules and are petrographically distinct (Adatte et al. 1996; Stinnesbeck et al. 1996). Therefore, an impact origin appears to be the most reasonable explanation and is consistent with the interpretation of morphologically similar spherules in various K-T boundary sections that have been attributed to the Chicxulub impact on the Yucatán peninsula (Table 1 with references). Further constrains to the origin of spherules and fragments can be derived from their characteristic internal structures:

1. Schlieren, marl, carbonate inclusions, and the absence of microliths (rare exceptions exist, see below) may document the rapid and violent mixing of melt from different origins, contamination with (unmolten) lithic clasts, and rapid quenching (Stähle 1972; Engelhardt et al. 1995; See et al. 1998). Such fast melting and cooling prevents the melt from homogenization and crystal growth (Glass 1990; Izett 1991). These features are characteristic of impact glasses (e.g., Stähle 1972; Glass 1990; Engelhardt et al. 1995; See et al. 1998; Dressler and Reimold 2001) and are rarely observed in volcanogenic pyroclasts (Fisher and Schmincke 1984; Cas and Wright 1987). Schlieren are also a prominent feature of "type 1" spherules from the K-T transition in Beloc, Haiti, though these schlieren are distinct in terms of their Ca- and S-enrichment (e.g., Izett 1991; Bohor and Glass 1995; Stüben et al. 2002).
2. Microliths are interpreted as devitrification products that developed during somewhat slower cooling (Shelley 1993). Despite the fact that they are now pseudomorphically replaced by calcite or chlorite, their characteristic shapes may constrain their initial mineralogy. We can distinguish between (a) thin skeletal and branching crystals that are similar to pyroxene and olivine textures observed in quenched mafic melts by laboratory experiments as well as in impact glasses of mafic composition (Jones et al. 2000;

Hörz and See 2000), (b) characteristic criss-cross patterns with twinned individuals, similar to quenched K-feldspar (Shelley 1993), and (c) dark radial hair-like crystals, analogous to pyroxene whiskers observed in impact glass from the Ries crater (Stähle 1972; Engelhardt et al. 1995). Such microliths have rarely been observed in "type 1" spherules from the K-T transition in other localities (e.g., Izett 1991; Bohor and Glass 1995), but are characteristic features of "type 2" spherules from the K-T boundary clay layer (e.g., Montanari 1991; Martínez-Ruíz et al. 1997; Smit 1999).

3. Globules enriched in Fe and Mg may be interpreted as exsolution or segregation of distinct phases in the melt, according to similar observations in igneous rocks (e.g., Philpotts 1990) and impact glasses (Delano and Hanson 1996). Their elongated and twisted forms argue against an exclusive diagenetic origin. Such immiscible melt globules might have been stretched by flow movements of the melt and suggest that quenching preceded completion of the mixing process (Delano and Hanson 1996). They are unique to spherules from the La Sierrita area and have not been discovered in other K-T localities to date.
4. Hematite, in part with a slight Si- and Ni-enrichment, formed either primarily from melt or as a replacement product of cubic minerals such as magnetite or pyrite during diagenesis (Philpotts 1990). The presence of garland–shaped, Ti- and Fe-rich lamellae, with crystal sizes of rutile and Ti-Fe oxide phases growing towards the interior of grains, and the dendritic or skeletal Ti-Fe oxide crystals with spinifex textures may indicate a primary origin by quenching from melt (Bryan 1972; Shelley 1993).

**Carbonate clasts** and **carbonate in spherules and fragments** expose a range of petrological textures (e.g., radially oriented needle-like calcite crystals) that may be attributed to diagenetic processes such as inorganic carbonate precipitation (e.g., Tucker and Wright 1992). However, several additional observations are difficult to reconcile with an exclusive diagenetic origin of these carbonates: (1) individual calcite globules are confined to the spherule deposits and show no traces of later infilling by diagenesis. (2) The 'emulsion-like' textures of carbonate intermingling with spherules and fragments. (3) The occurrence of coalesced calcite globules within spherules and fragments. (4) The presence of curved concave-convex menisci with sharp boundaries between spherules, fragments, and carbonate overgrowths or inclusions. (5) These textures are interrupted along fractures of broken spherules, fragments, and carbonates, and therefore appear to predate diagenesis. According to petrologic and experimental data provided by Graup (1999), Jones et al. (2000), and Osinski et al. (2001), these microtextures are indicative of liquid immiscibility with silicate melt and large parts of the calcite initially being in a liquid state. The carbonate overgrowths on spherules and fragments with radially aligned elongate, needle-like calcite crystals ('feathery calcite') are in line with this interpretation as they may attest to rapid cooling from a carbonate melt. Carbonates with similar textures have been found in suevite from the Ries crater, Germany (Graup 1999), the Haughton crater, Canada (Martinez et al. 1994; Graup 1999; Osinski and Spray 2001), and the Chicxulub crater (Jones et al. 2000). Evidence for a volcanic origin is generally restricted to carbonatites and alkali-basaltic volcanism (e.g., Philpotts 1990; Graup 1999).

In summary, and in line with the results of other studies on K-T boundary sections for comparable spherule deposits (Table 1 and references therein), we conclude that a multitude of distinct petrological features of spherules, fragments, and carbonate clasts from the La Sierrita area provides strong evidence for a common origin, an impact event, presumably from the Chicxulub crater on the Yucatán peninsula, southern Mexico. Compared to spherule deposits from other K-T localities, the amount of angular fragments is unusually high in the La Sierrita area. This might either be due to the proximity of La Sierrita to the Chicxulub crater (Glass et al. 1997), the inferred ejecta-dispersion mode (e.g., fluidization, see below), or due to subsequent rapid burial, resulting in good preservation of these deposits (e.g., slumping, see below). It is remarkable that, with the exception of marl and carbonate clasts, no lithic clasts with lower degrees of shock state (i.e., diaplectic glasses) have been observed, thus the spherule deposits appear to be entirely comprised of former liquid-state glasses and, hence, are indicative of "shock state IV", comprising shock pressures of 60–80 Gpa and postshock temperatures of 1,300–3,000 °C (Engelhardt et al. 1997; Montanari and Koeberl 2000). This impact melt was subsequently contaminated by ejected (molten and unmolten) carbonate and marl (micrite). The high amount of allochthonous carbonate clasts and globules points to a carbonate-rich target, supports an impact on a carbonate platform, and therefore strengthens the correlation between the spherule deposits in the La Sierrita area and the Chicxulub crater with its thick sequence of Cretaceous limestone, anhydrite, and gypsum (López-Ramos 1975; Ward et al. 1995). In combination with similar observations from other spherule deposits in Mexico (e.g., Smit et al. 1996; Jones et al. 2000), we stress that the dispersion of carbonate by the Chicxulub impact was substantial in this area, either as unshocked clasts or as melt.

### *Implications from geochemical phases*

The results from our mineralogical and geochemical analysis of spherules and fragments from the La Sierrita area suggest that they originally quenched from (impact-) melt(s) of predominantly mafic composition. The ubiquitous presence of secondary phases (e.g., chlorite, Fe-oxides, -hydroxides) is indicative of the pervasive submarine alteration of the former glass phase (see Fisher and Schmincke 1984; Berger et al. 1994; Mørk et al.

2001; Utzmann et al. 2002). Thereby, the chlorite may either have formed by direct replacement of the glass phase or of secondary phases such as Fe-, Mg-rich smectite or palagonite that replaced the glass during early diagenesis (e.g., Fisher and Schmincke 1984; Daux et al. 1994; Utzmann et al. 2002). These results are in contrast to morphologically similar spherules and fragments from other K-T boundary locations that differ significantly by their andesitic composition and have been interpreted as impact-generated mixtures of target lithologies currently known from the Yucatán peninsula, including sedimentary (carbonates, evaporites) and basement rocks (gneiss, tonalite, diabase dikes; e.g., Izett 1991; Bohor and Glass 1995). In order to explain these compositional differences, one may argue that, except for the mafic glass, this 'unusual' mafic composition is a (local) diagenetic artifact, and that the original composition of the La Sierrita area initially corresponded to the andesitic spherules found in other locations. However, we have accumulated evidence in favor of an initially different composition:

1. A progenitor of mafic composition is in line with the relict crystals in spherules and fragments, interpreted to be pseudomorphs of rapidly cooled pyroxene, feldspar, and olivine crystals.
2. Elements such as Ti, Al, and Fe are relatively insoluble in natural waters, and their amounts are therefore assumed to remain largely unchanged during rock alteration, though they are presumably entrapped in secondary phases, as observed in altered (basaltic) volcanic glasses (e.g., Crovisier et al. 1987; Daux et al. 1994; Stroncik and Schmincke 2002; Utzmann et al. 2002).
3. The excellent preservation of ejecta components with delicate microstructures including geochemically distinct internal domains (schlieren, globules) argues against a destructive diagenetic overprint that obliterated any primary geochemical signals. Moreover, severe penetrative alteration effects, if they have been active at all, would have affected all components including marl and carbonate clasts, consequently leading to a more homogeneous chemical composition and obliteration of inherited geochemical signals. However, these components are clearly distinguishable from the spherules and fragments, and show no specific enrichment in Fe, Mg, or Ti. In particular, isolated spherules and fragments, found in the silty limestone layer ('SLL') or sandstone of unit 2, show no compositional differences to their counterparts within the spherule deposits.
4. The Fe- and Mg-rich chlorite composition of spherules and fragments is apparently not a local phenomenon in the La Sierrita area: such spherule deposits are present in sections over a distance of more than 30 km (Affolter 2000; Schilli 2000). In addition, Fe-, K- and Mg-rich chlorite-smectite spherules and fragments have been reported also from El Peñon, La Lajilla, and El Mimbral, coincident with andesitic impact glass, smectites, and zeolites (Smit et al. 1992b; Stinnesbeck et al. 1993; Premo et al. 1995; Adatte et al. 1996; Kettrup 2002). According to Kettrup (2002), Fe- and Mg-rich chlorite spherules from La Lajilla show a similar trace element composition (Rb, Sr, Sm, Nd) and isotope ratios ($^{87}Sr/^{86}Sr$, $^{143}Nd/^{144}Nd$) to mafic Chicxulub impactites, which could give further evidence for a low degree of alteration.
5. No hydrothermal influx was recognized, nor has any been reported from elsewhere within the Méndez Formation that could explain the chloritization of spherules and fragments (Perez Cruz 1993).

We therefore conclude that alteration processes alone do not explain the compositional differences to otherwise morphologically similar spherules from other K-T locations. Consequently, we suggest that a significant contribution existed to the (impact-) melt from predominantly mafic target rocks as parental phases, though a contribution from intermediate to felsic target lithologies may also be present, as also revealed by the andesitic glasses and smectites found by Smit et al. (1992b), Stinnesbeck et al. (1993) and Adatte et al. (1996) at other NE Mexican sections. The good preservation of the eject components may be explained by carbonate cementation during early diagenesis that predated compaction by sediment overload (Mørk et al. 2001). The reason for the early cementation of these deposits may be that they were originally porous and permeable for fluid circulations; the large amount of carbonate clasts may have also acted as a major source for $Ca^{2+}$ and presumably promoted such processes.

Chicxulub impact melts are commonly regarded as derived exclusively from continental crust and platform-sediment lithologies with rare evidence for mafic target rocks from the Yucatán peninsula (e.g., Schuraytz et al. 1994). However, Sr/Nd isotopes of melt rocks from the Chicxulub crater and from glass and chlorite spherules from El Mimbral and La Lajilla led Premo et al. (1995), Kettrup et al. (2000), and Kettrup (2002) to assume the admixture of a mafic component (amphibolite?) from the Chicxulub impact site. Kring and Boynton (1992) reached a similar conclusion from their petrologic study of impact-melt rocks from Chicxulub; these authors proposed diabase, pyroxenite, or amphibolite as possible additional source rocks. These lithologies are known from the southeastern part of the Gulf of Mexico (e.g., DSDP Leg 77, Schlager et al. 1984). Therefore, we consider the possibility that such mafic rocks from the northern part of Yucatán contributed to the impact melt that generated the La Sierrita spherules and fragments, although a close assignation to a particular rock type is difficult for two reasons: (1) due to phase transformations during alteration, as outlined above, and (2) due to mixing and fractionation processes within the impact melt as observed at various impact craters as well as for distal ejecta from the K-T boundary impact (Attrep et al. 1991; Mittlefehldt et al. 1992; Evans et al. 1995; Hörz et al. 1998; See et al. 1999; Koeberl 1998; Dressler and

Reimold 2001). According to these authors, such mixing and fractionation processes may lead to compositional changes that are not correlated directly to specific target rock melts. The presence of Fe-, Ti-, and K-rich schlieren in spherules and fragments with element enrichments up to 25 and 12 wt%, respectively, may document such processes. It is difficult to judge whether these mixing and fractionation processes can also account for the remarkable high amount of Fe and Mg. The two are apparently positively correlated, thus suggesting a common source. One possible explanation could be the preferential melting of ferromagnesian minerals (Koeberl et al. 1994). Alternatively, the high Fe and Mg contents of spherules and fragments may be due to contribution from the presumably chondritic Chicxulub projectile, analogous to the interpretation of a distinct Fe and Mg enrichment in impact melts of the Kalkop impact crater, South Africa (Koeberl et al. 1994). Some of our observations point to the possibility of such a meteoritic contamination: (1) tiny metallic or sulfidic Ni- and Co-rich inclusions may indicate contamination from meteoritic material as refractory grains or condensed droplets; these elements are commonly concentrated in extraterrestrial matter (see Grieve et al. 1980; Koeberl 1998; Hart et al. 2002). (2) Contribution from extraterrestrial material could also account for the Ni-enrichment within hematite crystals that is rather unusual for hematite of diagenetic origin. Ni-rich iron oxides have also been reported by Soria et al. (2001) for spherules of the La Sierrita area, as well as from "type 2" spherules from the K-T boundary clay (e.g., Doehne and Margolis 1990; Montanari 1991; Martínez-Ruíz et al. 1997; Bauluz et al. 2000; Claeys et al. 2002). However, due to our petrological results, both types of inclusions constitute only a minute component, as additionally revealed by the trace element analyses of bulk samples, which showed no significant enrichment in these siderophile elements. Therefore, the presence of an extraterrestrial component in spherules and fragments can be considered as a possibility, though our data provide no definitive answer, in particular in the absence of PGE or Cr-, Os-isotopic data and without a definite knowledge of the target rock petrology.

Taking into account a potential contribution from mafic target rocks, it is remarkable that the petrological and mineralogical characteristics of the La Sierrita spherules and fragments bear an overall resemblance to the "type 2" spherules that are found in the K-T boundary clay layer in sections in the Atlantic, Pacific, and Tethyan realm (Doehne and Margolis 1990; Smit and Klaver 1981; Montanari 1991; Smit et al. 1992a; Bohor and Glass 1995; Martínez-Ruíz et al. 1997; Bauluz et al. 2000; Claeys et al. 2002; Verma et al. 2002). These "type 2" spherules are compositionally highly variable and consist of hematite, goethite, magnetite, pyroxene, smectite, and K-feldspar, and frequently include Ni-, Cr-rich spinels. In contrast to the andesitic "type 1" spherules, the "type 2" spherules are interpreted to have originated either from mafic target rocks (oceanic crust?) and/or from the (Chicxulub) impactor, analogous to the enclosing basal portion of the K-T boundary clay (Smit and Klaver 1981; Schmitz 1988, 1992; Montanari 1991; Bohor and Glass 1995; Martínez-Ruíz et al. 1997; Ortega-Huertas et al. 1998; Bauluz et al. 2000; Wdowiak et al. 2001).

## Depositional and deformational processes

The lithological characteristics and spatial relationships of spherule deposits in the La Sierrita area suggest diverse interacting sedimentary processes that operated on a local to regional scale. These processes are not easily resolved with the limited outcrop data and in the absence of distinct bedding features in the uniform Méndez marls. To distinguish between initial and superimposed depositional processes, we combined microfacies and outcrop data.

### *Implications from microfacies*

**Type 1 microfacies** with loosely packed welded or clustered components exhibiting random grain orientation, poor sorting, and absence of grading suggest an origin of these deposits as rapidly settled air-water fallout-ejecta, presumably winnowed and redistributed by diluted turbidity currents (Cas and Wright 1987; Bitschene and Schmincke 1991; d'Atri et al. 1999). The absence of lateral flow indicators such as alignment of platy fragments, cross-bedding as well as the absence of abrasion features and sorting for these components supports this interpretation and argues against long-term transport on the sea floor by either high-energetic submarine currents or within grain- and debris-flows (Bitschene and Schmincke 1991; d'Atri et al. 1999). This interpretation is also consistent with the occurrence of this microfacies in the interchannel area (as primary fallout?) and in the channel margin to levee area, where low-density turbidity currents may have redistributed them locally. In addition, the good preservation of fabric, the high amount of spar cement, and the absence of bioturbation, as well as omission surfaces in these deposits suggest rapid syn- or postdepositional burial.

The characteristic welding and amalgamation of spherules and fragments as well as the enveloping of carbonate clasts, marl, and benthic foraminifera, could have resulted from compaction by sediment overload (Tucker and Wright 1992; Collinson 1994; Bohor 1996). The majority of these particles, however, show a random grain orientation with their long axes not aligned parallel to the bedding. Combined with the three-dimensional mesh-like fabric, abundant pore space, and good preservation of components, this suggests that these structures originated in a ductile state before cooling (Cas and Wright 1991; Kokelaar and Busby 1992; Freundt and Schmincke 1998). Transport and emplacement as hot ejecta on the sea floor at high temperatures is unlikely, due to the paleowater depth of 300–1,000 m (Alegret et al. 2001; Soria et al. 2001; Keller et al. 2002b) and the

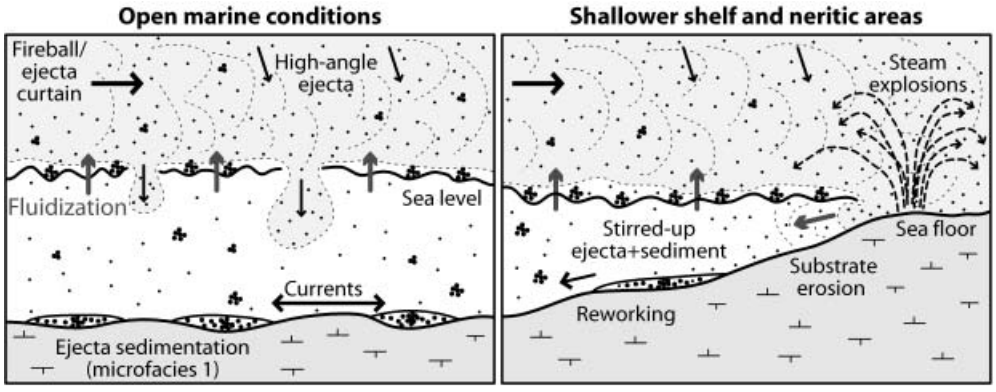


**Fig. 11** Conceptual sketch based on the hypothesis that the ejecta curtain behaves similar to a pyroclastic flow. It demonstrates the initial ejecta-dispersion by the vapor-rich ejecta curtain, gliding over the sea and entering shallower marine settings, causing large steam explosions; modified after Cas and Wright (1991) and Freundt and Schminke (1998)

small thickness of the deposit (e.g., Cas and Wright 1991). Therefore, another mechanism is required to account for these features: one possible scenario for ejecta dispersion combined with amalgamation and welding of components incorporates the generation of a hot, fluidized and outward radiating curtain of molten ejecta, entrained clasts, vapor, and admixed seawater by the impact (Alvarez et al. 1995). This 'ejecta curtain' may behave analogous to a volcanic-generated pyroclastic flow and may be transported over long distances on top of the sea surface as depicted in Fig. 11 (e.g., Cas and Wright 1991; Ormö and Lindström 2000). Such a ground surge-like transportation mechanism could account for the wide distribution of such coarse ejecta more than five crater radii from the Yucatán peninsula (Cas and Wright 1991; Ormö and Lindström 2000; Sturkell et al. 2000). Finally, this ejecta-dispersion mode could also account for the incorporation of marl and benthic foraminifera by erosion of shallower areas of the Mexican shelf and mixing with the hot ejecta, presumably enhanced by steam-explosions during entry in shallower areas, as observed for pyroclastic flows (e.g., Freundt and Schminke 1998). Benthic foraminifera observed in this microfacies type include *Anomalina*, *Cibicidoides*, *Lenticulina*, *Neoflabellina*, *Tritaxia*, and *Palmula*, which are not characteristic carbonate-platform occupants (Murray 1991). Analogous to observations from other marine impact structures, subsequent resurge currents presumably contributed to the redistribution of settling ejecta towards offshore areas (McHugh et al. 1998; Ormö and Lindström 2000; Dalwigk and Ormö 2001).

**Type 2 microfacies** represents a mixture of spherules, fragments, carbonate clasts and large outsized marl clasts in a marly matrix without sedimentary structures such as grading or alignment of clasts, thus arguing against a primary fallout origin of these layers. Consequently, they are interpreted to be remolded spherule deposits that were mixed with Méndez marls by soft-sediment deformation processes (e.g., Bitschene and Schmincke 1991; d'Atri et al. 1999; Stix 1991). This interpretation is supported by the occurrence of this microfacies either within the channelized facies as local reworked marl clast/spherule breccia, or in the nonchannelized facies where soft sedimentary processes included slumping, sliding, or liquefaction (see below).

**Type 3 microfacies** consist of spherules, fragments and carbonate clasts, in addition to minor, but variable amounts of siliciclastic detritus; these components are rarely orientated or graded and welding features are generally absent. Therefore, these deposits do not appear to be primary fallout deposits, but are rather the result of local reworking and dissemination of ejecta by turbidite currents or debris flows, accompanied by contamination with terrigeneous detritus (e.g., Bitschene and Schmincke 1991; Stix 1991; d'Atri et al. 1999). However, the complete lack of significant abrasion, sorting, and the preservation of delicate ejecta components implies short transport that is difficult to reconcile with the more long-term transport of the siliciclastic detritus that presumably derived from proximal shelf or coastal areas. A possible explanation could be that strong basinward directed submarine currents carried sand in turbulent suspension or within debris flows from nearshore or shallow shelf areas and incorporated surficial nonconsolidated ejecta deposits from areas close to La Sierrita along their pathway. The incorporation of surficial ejecta deposits is also indicated by the similar mineralogical and geochemical composition of the microfacies type 1 and 3 spherule deposits, arguing against intense mixing with Méndez marls (Fisher and Schmincke 1984; Cas and Wright 1987; Johansson and Stow 1995; d'Atri et al. 1999). This interpretation is consistent with the occurrence of these deposits at the base of the sand-siltstone complex in the channel axis area.

### *Implications from stratigraphy and lithology*

In the northern La Sierrita area, **spherule deposits interbedded in Méndez marl** constitute isolated and lenticular units of either: (1) contorted and recumbent folded layers with curvilinear fold hinges that bear characteristic outsized marl clasts (armored by spherules) in their cores, or (2) disaggregated (breccia-like) spherule deposits of chaotic appearance that occur in close proximity to the folded deposits. According to the criteria provided by Martinson (1994), Mulder and Cochonat

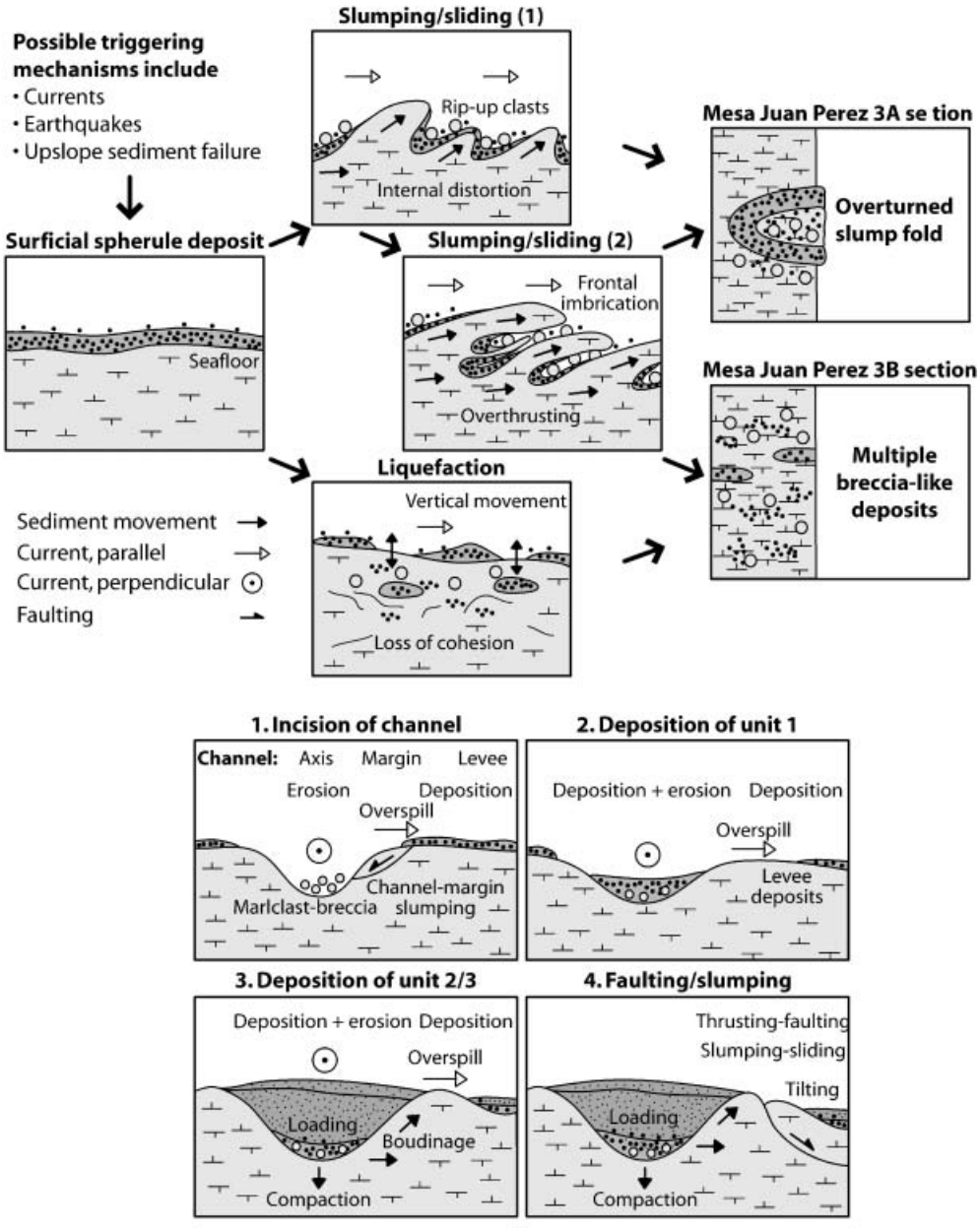


**Fig. 12a, b** Schematic model demonstrating the supposed generation and related sedimentological features of **a** slump-folded and sedimentary breccia-like deposits and **b** channelized deposits in the La Sierrita area; modified after Corbett (1973), Maltman

(1996), and Hampton et al. (1997), these sedimentary features are indicative of downslope sediment movements associated with soft-sediment deformation (see also Soria et al. 2001). The contorted and recumbent folded deposits are interpreted as coherent to semi-coherent slump structures (Corbett 1973; Elliot and Williams 1988; Martinsen 1994). The characteristic outsized marl clasts in their cores may have been derived from up-slope directed parts of the slump sheet and point to the presence of erosive high-energy currents, presumably associated with the slumping of these beds. This indicates that in these localities, spherule deposits were not entirely buried by sediments before slumping took place and, therefore, slumping likely affected superficial spherule deposits ("open-cast slumps", Corbett 1973). The 'breccia-like' appearance of the spherule deposits may indicate local acceleration of the slumps down-slope into a sedimentary mass flow-slide, in which internal cohesion is lost (Corbett 1973; Elliot and Williams 1988; Guiraud and Plaziat 1993; Martinsen 1994). Likewise, they may be interpreted as the result of liquefaction of marls and spherule layers (Decker 1990; Nichols 1995). Both sliding, as well as liquefaction, is indicative of penecontemporaneous deformation preceding lithification (Elliot and Williams 1988); these processes are schematically depicted in Fig. 12a.

Considering the small scale of the soft-sediment mass movements in the La Sierrita area, we conclude that the lens-like and irregular shapes of spherule deposits within Méndez marls and their limited lateral correlation in

between outcrops some 10 m apart indicates local phenomena, rather than truly sheet-like (Corbett 1973). The vertical extension of intermittent breccia-like spherule deposits in the Mesa Juan Perez 3 section suggests that soft sediment deformation and mass movements may have affected the upper 4–8 m of the Méndez marls in the La Sierrita area (see Fig. 4). These characteristics combined with the relative 'integrity' of deformed spherule layers advocates for a minor transportation distance (tens to hundreds of meters?) of slumps or slides (Maltman 1994b; Martinsen 1994), which is in contrast to the "continental slope failure" suggested by Soria et al. (2001). However, the limited outcrop scale, the vertical offset between outcrops, and the absence of distinct glide planes in the almost structureless Méndez marls do not allow for further evaluation of size and extension of the slump or slide masses.

The cause(s) of these sedimentary mass movements are difficult to establish, though such rapidly deposited and coarse-grained deposits are particularly susceptible to soft-sediment disturbances (e.g., Collinson 1994), and the paleobathymetric outer shelf to bathyal setting of the La Sierrita area (Alegret et al. 2001; Soria et al. 2001; Keller et al. 2002b) presumably promoted these processes (e.g., Shanmugam et al. 1994; Hampton et al. 1997). In the Maria de los Angeles 1 and the Mesa Juan Perez 3A sections, the slump fold axis roughly parallels the assumed direction of the paleoslope (inclined towards SSE, Perez Cruz 1993; Keller et al. 1994; Bohor 1996) and the inferred current direction of the sandstones, thus pointing to gravity- or current-driven processes. Considering the suggested outer shelf to bathyal setting of these deposits, well below storm wave-base, seismic shaking, strong bottom currents, or upslope sediment failure could be plausible trigger mechanisms (e.g., Morton 1993; Maltman 1994a; Stow et al. 1996; Hampton et al. 1997).

It appears unlikely that these triggering mechanisms were directly associated with the ejecta generation by the Chicxulub impact, because they affected 'thick' ejecta deposits with ejecta that has already traveled several hundred meters through the water column. Further evidence for soft-sedimentary mass-movements of spherule deposits has so far only been reported from Beloc, Haiti, (e.g., Keller et al. 2001; Fig. 1), though attributed to local synsedimentary tectonic events by these authors. However, large scale slumping of Maastrichtian sediments underlying (and locally affecting) spherule deposits, and ascribed to seismic shaking by the Chicxulub impact was reported from the Western Atlantic margin at the Blake Nose Plateau and the Bermuda Rise (Klaus et al. 2000; Norris et al. 2000; Norris and Firth 2002).

The variable lithology of **spherule deposits at the base of the sand-siltstone sequence** (unit 1), and their regional persistence and local impersistence, channelized geometry, scoured basal contact, as well as absence of grading imply deposition from multiple phases of channelized debris flow chutes or turbidity currents of variable density under high flow regimes (e.g., Martinsen 1994; Johansson and Stow 1995; Mulder and Cochonat 1996; Stow et al. 1996; Stow and Mayall 2000). The localized marl clast breccias and outsized marl clast point to deposition by erosive high-velocity currents and may have been generated by the undercutting and erosion of channel margins, causing intra-, extrachannel slumping and sliding (Shanmugam et al. 1994; Johansson and Stow 1995; Mulder and Cochonat 1996; Stow and Mayall 2000). The detritus content and the embedded sandstone layers suggest influx from nearshore or more proximal shelf areas. In contrast, spherule deposits from the channel margin levee area (comprising microfacies type 1) show no terrigeneous enrichment and were presumably deposited under low to moderate flow regimes by low-density turbidity currents. A schematic model for the generation of these channels is depicted in Fig. 12b. Current-induced sedimentary mass movement processes and, in particular, transport by debris flows or turbidity currents have previously been proposed for spherule deposits from numerous K-T sections in the Gulf of Mexico area (e.g., Beloc, Haiti; Brazos, Texas; Mimbral, NE Mexico; see Table 1 for references). These papers also discuss potential causal mechanisms for these sedimentary mass movements, including impact-induced tsunamis or turbidites, or the Late Maastrichtian sea-level lowstand.

The tilting, boudinage, and lateral movement ('squeezing') of unit 1 spherule deposits in the Mesa Juan Perez 1A and in the El Toro section, may have been induced by loading with the up to 10-m(!)-thick sand-siltstone complex. Such loading may have also caused local relief adjacent to the channel, thus resulting in destabilization of channel margin-levee areas associated with later, secondary mass movements and/or faulting as observed at the Maria de los Angles 1C section, where the slump fold axis parallels the channel axis of the sand-siltstone complex. Such secondary mass movements may provide an explanation for the apparent vertical dislocation between parts of the sand-siltstone deposit against each other by up to 10 m, in the Mesa Juan Perez and the Maria de los Angeles area, where preferentially the channel margin-levee area was moved down relative to the channel axis (e.g., in the sections with multiple spherule deposits). Likewise, differential compaction (marl vs. sand-siltstone) may have caused or enhanced this vertical offset (Johansson et al. 1998).

### *Relationship to other spherule deposits in NE Mexico*

Numerous spherule deposits have been discovered in northeastern Mexico at the base of the sand-siltstone deposit (see Table 1 for references) and three to four spherule deposits are locally interbedded in Mendez marls with no evidence of major folding or slumping (Stinnesbeck et al. 2001; Keller et al. 2002a, 2002b), though local small-scale slumps have been reported (see above and Soria et al. 2001, 2002). In the Loma Cerca section described by Stinnesbeck et al. (2001) and Keller et al. (2002b), Méndez marls are interpreted to show normal

pelagic deposition between spherule deposits, as indicated by the characteristic succession of planktic foraminiferal assemblages, and deposition occurred over time within biozone CF1 (*P. hantkeninoides* zone) which spans the last 300 ka of the Maastrichtian. In this section, reworking appears to be primarily restricted to the middle and topmost spherule deposits, with no evidence of reworking in the lowermost spherule deposit. However, evaluation of the biostratigraphic position of these units with respect to the K-T boundary is beyond the scope of this paper. In consequence, the reader is referred to the discussion provided by Stinnesbeck et al. (2001) and Keller et al. (2002a, 2002b) who suggested a pre-K-T impact with the deposition of the original spherule deposit at the base of biozone CF1. Contrary to this scenario, Soria et al. (2001, 2002) suggested a short-term scenario for Chicxulub ejecta deposition and subsequent slumping/gravity flows immediately at the K-T boundary. The importance of the slumped and channelized spherule deposits described here, is in the excellent preservation of ejecta, probably as a result of rapid burial, and its unusual mafic composition, which provides further clues to the Chicxulub pre-impact lithology.

## Conclusions

1. In the northern La Sierrita area, spherule deposits are locally embedded in late Maastrichtian marls and have been affected by remolding and reworking due to slumps-slides, liquefaction, and debris flows subsequent to original deposition. The laterally more widespread spherule deposits at the base of a sand-siltstone complex are interpreted as the result of confined channelized debris flows or turbidites with incorporation of terrigeneous influx from proximal shelf areas.
2. Spherule deposits consist of mm–cm-sized spherical to drop-shaped vesiculated spherules, angular to filamentous (ejecta-) fragments and abundant carbonate. Multiple morphological and petrological features (e.g., shapes, schlieren) of spherules and fragments, and the presence of carbonate with microtextures indicative of quenching and/or liquid immiscibility, as well as the close proximity of the La Sierrita area to the Yucatán peninsula indicate that the spherule deposits most likely originated as ejecta from the Chicxulub impact event. Petrological, mineralogical, and geochemical criteria suggest that ejecta components from the various spherule deposits are similar, with multiple deposits produced by remolding and reworking, though size sorting and abrasion of ejecta has not been observed. Welded and amalgamated ejecta constituents as well as enveloping of marl and benthic foraminifera by ejecta particles suggest an initial ground surge-like dispersion of the ejecta.
3. Spherules correspond morphologically to glassy and smectitic spherules of andesitic composition found in the K-T transition in the Gulf of Mexico and adjacent areas. However, at La Sierrita, spherules and fragments are distinct by their mafic geochemistry with high Fe, Al, and Mg, and low Si values and the presence of K-rich mafic glass. They contain Ti-, Fe-, K-rich schlieren, Fe-, Mg-rich globules, and rare µm-sized metallic and sulfidic Ni-, Co-rich inclusions. Although possible ejecta-fractionation or -mixing processes and alteration make accurate evaluation difficult, this suggests that they originated from mafic lithologies, in addition to a contribution from intermediate-felsic rocks and the possibility of meteoritic contamination.

**Acknowledgements** This work is part of the first author's PhD thesis, which was supported by the German Science Foundation (grants STI 128/7-1 to 2 and STU 169/10-2). We thank Jose G. López-Oliva, Falk Lindenmaier, and Armin Schafhauser for discussions and support during fieldwork in Mexico. We also thank Robert Speijer for identification of benthic foraminifera, Volker Zibat for assistance in electron microprobe analyses, and Stephan Unrein for preparation of thin sections. This paper benefited from discussions with Günther Graup, Jörg Keller, Jonas Kley, and Agnes Kontny. We appreciate constructive reviews by Philippe Claeys and Christian Koeberl.

## References

Adatte T, Stinnesbeck W, Keller G (1996) Lithostratigraphic and mineralogic correlations of near K/T boundary clastic sediments in NE Mexico: Implications for origin and nature of deposition. In: Ryder G, Fastovsky D, Gartner S (eds) The Cretaceous-Tertiary boundary event and other catastrophes in Earth history. Geol Soc Am Spec Pap 307:211–226

Affolter M (2000) Etude des depots clastiques de la limite Cretace-Tertiare dans la région de la Sierrita, Nuevo Leon, Mexique. Unpublished master Thesis, Université de Neuchâtel, 133 pp

Alegret L, Molina E, Thomas E (2001) Benthic foraminifera at the Cretaceous-Tertiary boundary around the Gulf of Mexico. Geology 29:891–894

Alvarez W, Claeys P, Kieffer SW (1995) Emplacement of Cretaceous-Tertiary boundary shocked quartz from Chicxulub crater. Science 269:930–935

Arz JA, Arenillas I, Soria AR, Alegret L, Grajales-Nishimura JM, Liesa CL, Melendez A, Molina E, Rosales MC (2001) Micropaleontology and sedimentology across the Cretaceous/Tertiary boundary at La Ceiba (Mexico): impact-generated sediment gravity flows. J S Am Earth Sci 14:505–519

Attrep M, Orth CJ, Quintana LR, Shoemaker CS, Shoemeker EM, Taylor SR (1991) Chemical fractionation of siderophile elements in impactites from Australian meteorite craters (abstract). Lun Planet Sci 22:39–40

Bailey SW (1988) Chlorites: Structures and crystal chemistry. In: Bailey SW (ed) Hydrous phyllosilicates (exclusive of micas) reviews in mineralogy. Mineralogical Society of America, pp 347–403

Barrera E, Savin SM (1999) Evolution of late Campanian-Maastrichtian marine climates and oceans. In: Barrera E, Johnson CC (eds) Evolution of the Cretaceous ocean-climate system: Geol Soc Am Spec Pap 332:245–282

Bauluz B, Peacor DR, Elliott WC (2000) Coexisting altered glass and Fe/Ni oxides at the Cretaceous/Tertiary boundary, Stevns Klint (Denmark): direct evidence of meteorite impact. Earth Planet Sci Lett 182:127–136

Berger G, Claparols C, Guy C, Daux V (1994) Dissolution rate of a basalt glass in silica-rich solutions: implications for long-term alteration. Geochim Cosmochim Acta 58:4875–4886

Bitschene PR, Schmincke H-U (1991) Fallout tephra layers: composition and significance. In: Heling D, Rothe P, Förster U et al. (eds) Sediments and environmental geochemistry. Springer, Berlin Heidelberg New York, pp 48–82
Bohor BF (1996) A sediment gravity flow hypothesis for siliciclastic units at the K/T boundary, northeastern Mexico. In: Ryder G, Fastovsky D, Gartner S (eds) The Cretaceous-Tertiary boundary event and other catastrophes in Earth history: Geol Soc Am Spec Pap 307:183–195
Bohor BF, Betterton WJ (1989) Glauconite spherules and shocked quartz at the K-T boundary in DSDP Site 603 B (abstract). Lun Planet Sci 20:92–93
Bohor BF, Glass BP (1995) Origin and diagenesis of K/T impact spherules—from Haiti to Wyoming and beyond. Meteoritics 30:182–198
Bohor BF, Triplehorn DM, Nichols DJ, Millard HTJ (1987) Dinosaurs, spherules, and the "magic" layer: A new K-T boundary clay site in Wyoming. Geology 15:896–899
Bourgeois J, Hansen TA, Wiberg P, Kauffman EG (1988) A tsunami deposit at the Cretaceous-Tertiary boundary in Texas. Science 141:567–570
Bromley RG (1996) Trace fossils: Biology, taphonomy and applications. Chapman and Hall, London
Bryan WB (1972) Morphology of quench crystals in submarine basalts. J Geophys Res 77:5812–5819
Cas RAF, Wright JV (1987) Volcanic successions, modern and ancient: a geological approach to processes, products and successions. Allen and Unwin, London
Cas RAF, Wright JV (1991) Subaqueous pyroclastic flows and ignimbrites: an assessment. Bull Volcanol 53:357–380
Claeys P, Kiessling W, Alvarez W (2002) Distribution of Chicxulub ejecta at the Cretaceous-Tertiary boundary. In: Koeberl C, MacLeod KG (eds) Catastrophic events and mass extinctions: impacts and beyond. Geol Soc Am Spec Pap 356:55–68
Clark JD, Pickering KT (1996) Submarine channels: processes and architecture. Vallis Press, London
Collinson JD (1994) Sedimentary deformation structures. In: Maltman AJ (ed) The geological deformation of sediments. Chapman and Hall, London, pp 95–125
Corbett KD (1973) Open-cast slump sheets and their relationship to sandstone beds in an upper Cambrian flysch sequence, Tasmania. J Sediment Petrol 43:147–159
Covey C, Thompson SL, Weissman PR, MacCracken MC (1994) Global climatic effects of atmospheric dust from an asteroid or comet impact on Earth. Global Planet Change 9:263–273
Crovisier JL, Honnorez J, Eberhart JP (1987) Dissolution of basaltic glass in seawater: Mechanism and rate. Geochim Cosmochim Acta 51:2977–2990
Perez Cruz GAP (1993) Geologic evolution of the Burgos basin, Northeastern Mexico. PhD Thesis, Rice University, 155 pp
d'Atri A, Dela Pierre F, Lanza R, Ruffini R (1999) Distinguishing primary and resedimented vitric volcaniclastic layers in the Burdigalian carbonate shelf deposits in Monferrato (NW Italy). Sediment Geol 129:143–163
Dalwigk Iv, Ormö J (2001) Formation of resurge gullies at impacts at sea: the Lockne crater, Sweden. Meteor Planet Sci 36:359–369
Daux V, Crovisier JL, Hemond C, Petit JC (1994) Geochemical evolution of basaltic rocks subjected to weathering: fate of the major elements, rare earth elements, and thorium. Geochim Cosmochim Acta 58:4941–4954
Decker PL (1990) Style and mechanics of liquefaction-related deformation; lower Absaroka Volcanic Supergroup (Eocene), Wyoming. Geol Soc Am Spec Pap 240:71
Delano JW, Hanson B (1996) Liquid immiscibility: Cause of compositional heterogeneity in tektites (abstract). Lun Planet Sci 27:305–306
Doehne E, Margolis SV (1990) Trace-element geochemistry and mineralogy of the Cretaceous/Tertiary boundary: identification of extraterrestrial components. In: Sharpton VL, Ward PD (eds) Global catastrophes in Earth history: an interdisciplinary conference on impacts, volcanism, and mass mortality. Geol Soc Am Spec Pap 247:367–382
Dressler BO, Reimold WU (2001) Terrestrial impact melt rocks and glasses. Earth-Sci Rev 56:205–284
Ekdale AA, Stinnesbeck W (1998) Trace fossils in Cretaceous-Tertiary (KT) boundary beds in Northeastern Mexico: implications for sedimentation during the KT boundary event. Palaios 13:1–23
Elliot CG, Williams PE (1988) Sediment slump structures: A review of diagnostic criteria and application to an example from Newfoundland. J Struct Geol 10:171–182
Engelhardt Wv, Arndt J, Fecker B, Pankau HG (1995) Suevite breccia from the Ries crater, Germany: Origin, cooling history and divitrification of impact glasses. Meteoritics 30:279–293
Engelhardt Wv, Arndt J, Fecker B, Pankau HG (1997) Suevite breccia from the Ries impact crater, Germany: Petrography, chemistry and shock metamorphism of crystalline rock clasts. Meteor Planet Sci 32:545–554
Evans NJ, Ahrens TJ, Gregoire DC (1995) Fractionation of ruthenium from iridium at the Cretaceous-Tertiary boundary. Earth Planet Sci Lett 134:141–153
Fisher RV, Schmincke H-U (1984) Pyroclastic rocks. Springer, Berlin Heidelberg New York
Freundt A, Schmincke H-U (1998) Emplacement of ash layers related to high-grade ignimbrite P1 in the sea around Gran Canaria. In: Weaver PPE, Schmincke H-U, Firth JV et al. (eds) Proceedings of the Ocean Drilling Program, Scientific Results 157. Ocean Drilling Program, College Station, Texas, pp 201–218
Glass BP (1990) Tektites and microtektites: key facts and inferences. Tectonophysics 171:393–404
Glass BP, Muenow DW, Bohor BF, Meeker GP (1997) Fragmentation and hydration of tektites and microtektites. Meteor Planet Sci 32:333–341
Graup G (1981) Terrestrial chondrules, glass spheres and accretionary lapilli from the suevite, Ries Crater, Germany. Earth Planet Sci Lett 55:407–418
Graup G (1999) Carbonate-silicate liquid immiscibility upon impact melting: Ries Crater, Germany. Meteor Planet Sci 34:425–438
Grieve RAF, Palme H, Plant AG (1980) Siderophile-rich particles in the melt rocks at the E. Clearwater Impact structure, Quebec: their characteristics and relationship to the impacting body. Contrib Mineral Petrol 75:187–198
Guiraud M, Plaziat J-C (1993) Seismites in the fluviatile Bima sandstones: Identification of paleoseisms and discussion of their magnitudes in a Cretaceous synsedimentary strike-slip basin (Upper Benue, Nigeria). Tectonophysics 225:493–522
Gupta SC, Ahrens TJ, Yang W (2001) Shock-induced vaporization of anhydrite and global cooling from the K/T impact. Earth Planet Sci Lett 188:399–412
Hallam A, Wignall PB (1999) Mass extinctions and sea-level changes. Earth-Sci Rev 48:217–250
Hampton MA, Lee HJ, Locat J (1997) Submarine landslides. Rev Geophys 34:33–59
Hansen T, Farrell BR, Upshaw III B (1993) The first 2 million years after the Cretaceous-Tertiary boundary in east Texas: rate and paleoecology of the molluscan recovery. Paleobiology 19:251–265
Hart RJ, Cloete M, McDonald I, Carlson RW, Andreoli MAG (2002) Siderophile-rich inclusions from the Morokweng impact melt sheet, South Africa: possible fragments of a chondritic meteorite. Earth Planet Sci Lett 198:49–62
Heymann D, Yancey TE, Wolbach WS, Thiemens MH, Johnson EA, Roach D, Moecker S (1998) Geochemical markers of the Cretaceous-Tertiary boundary event at Brazos River, Texas, USA. Geochim Cosmochim Acta 62:173–181
Hörz F, See TH (2000) Quenched olivines and pyroxenes in impact melts from Meteor Crater, AZ (abstract). Lun Planet Sci 31:#1737 (CD-ROM)
Hörz F, See TH, Yang V, Mittlefehldt DW (1998) Major element composition of ballistically dispersed melt particles from

Meteor Crater, AZ (abstract). Lun Planet Sci 29:#1777 (CD-ROM)
Ivanov BA, Badukov DD, Yakovlev OI, Gerasimov MV, Dikov YP, Pope KO, Ocampo AC (1996) Degassing of sedimentary rocks due to the Chicxulub impact: Hydrocode and physical simulations. In: Ryder G, Fastovsky D, Gartner S (eds) The Cretaceous-Tertiary boundary event and other catastrophes in Earth history: Geol Soc Am Spec Pap 307:125–139
Izett GA (1990) The Cretaceous/Tertiary boundary interval, Ration basin, Colorado and New Mexico, and its content of shock-metamorphosed minerals: evidence relevant to the K/T boundary impact-extinction event: Geol Soc Am Spec Pap 249:100
Izett GA (1991) Tektites in Cretaceous-Tertiary boundary rocks on Haiti and their bearing on the Alvarez impact extinction hypothesis. J Geophys Res 96:20879–20905
Johansson M, Stow DAV (1995) A classification scheme for shale clasts in deep water sandstones. In: Hartley AJ, Prosser DJ (eds) Characterization of deep marine clastic systems. Geol Soc Lond Spec Pub 94:221–241
Johansson M, Braakenburg NE, Stow DAV, Faugeres J-C (1998) Deep-water massive sands: facies, processes and channel geometry in the Numidian Flysch, Sicily. Sediment Geol 115:233–265
Jones AP, Claeys P, Heuschkel S (2000) Impact melting of carbonates from the Chicxulub impact crater. In: Gilmour I, Koeberl C (eds) Impacts and the early Earth. Lecture Notes in Earth Sciences 91. Springer, Berlin Heidelberg New York, pp 343–361
Keller G (1989) Extended period of extinction across the Cretaceous/Tertiary boundary in planktonic foraminifera of continental-shelf sections: Implications for impact and volcanism theories. Geol Soc Am Bull 101:1408–1419
Keller G (1996) The Cretaceous/Tertiary mass extinction in planktic foraminifera: Biotic constraints for catastrophe theories. In: MacLeod N, Keller G (eds) Cretaceous–Tertiary boundary mass extinction: biotic and environmental changes. Norton Press, New York, pp 49–84
Keller G, Stinnesbeck W, López-Oliva J-G (1994) Age, deposition and biotic effects of the Cretaceous/Tertiary boundary event at Mimbral, NE Mexico. Palaios 9:144–157
Keller G, López-Oliva J-G, Stinnesbeck W, Adatte T (1997) Age, stratigraphy and deposition of near-K/T siliciclastic deposits in Mexico: relation to bolide impact? Geol Soc Am Bull 109:410–428
Keller G, Adatte T, Stinnesbeck W, Stüben D, Berner Z (2001) Age, chemo- and biostratigraphy of Haiti spherule-rich deposits: A multievent K-T scenario. Can J Earth Sci 38:197–227
Keller G, Stinnesbeck W, Adatte T (2002a) Comment: Slumping and a sandbar deposit at the Cretaceous-Tertiary boundary in the El Tecolote section (northeastern Mexico): an impact-induced sediment gravity flow. Geology 30:382–383
Keller G, Adatte T, Stinnesbeck W, Affolter M, Schilli L, López-Oliva J-G (2002b) Multiple spherule layers in the late Maastrichtian of northeastern Mexico. In: Koeberl C, MacLeod KG (eds) Catastrophic events and mass extinctions: impacts and beyond: Geol Soc Am Spec Pap 356:145–162
Kettrup B (2002) Impact lithologies and target rocks of the impact craters Popigai, Russia, and Chicxulub, Mexico: Geochemical investigations. PhD Thesis, Westfälische Wilhelms Universität, Münster 88 pp
Kettrup B, Deutsch A, Ostermann M, Agrinier P (2000) Chicxulub impactites: geochemical clues to the precursor rocks. Meteor Planet Sci 35:1229–1238
Kiessling W, Claeys P (2001) A geographic database approach to the KT boundary. In: Buffetaut E, Koeberl C (eds) Geological and biological effects of impact events. Impact studies. Springer, Berlin Heidelberg New York, pp 83–140
Klaus A, Norris RD, Kroon D, Smit J (2000) Impact-induced mass wasting at the K-T boundary: Blake Nose, western North Atlantic. Geology 28:319–322
Klaver GT, Van Kempen TMG, Bianchi FR (1987) Green spherules as indicators of the Cretaceous/Tertiary boundary in Deep Sea Drilling Project Hole 603B. In: Van Hinte JE, Wise SW, Bianchi FR (eds) Initial Reports of the Deep Sea Drilling Project 93. US Governmental Printing Office, Washington, pp 1039–1047
Koeberl C (1998) Identification of meteoritic components in impacites. In: Grady MM, Hutchison R, McCall GJH et al. (eds) Meteorites: flux with time and impact effects. Geol Soc Lond Spec Pub 140:133–153
Koeberl C, Sigurdsson H (1992) Geochemistry of impact glasses from the K/T boundary in Haiti: relation to smectites and a new type of glass. Geochim Cosmochim Acta 56:2113–2129
Koeberl C, Reimold WU, Shirey SB, Le Roux FG (1994) Kalkkop crater, Cape Province, South Africa: confirmation of impact origin using osmium isotope systematics. Geochim Cosmochim Acta 58:1229–1234
Kokelaar P, Busby C (1992) Subaqueous explosive eruption and welding of pyroclastic deposits. Science 257:196–200
Kramar U (1997) Advances in energy-dispersive X-ray fluorescence. J Geochem Exploit 58:73–80
Kring DA, Boynton WV (1992) Petrogenesis of an augite-bearing melt rock in the Chicxulub structure and its relationship to K/T impact spherules in Haiti. Nature 358:141–143
Lerbekmo JF, Sweet AR, Davidson RA (1999) Geochemistry of the Cretaceous-Tertiary (K-T) boundary interval: south-central Saskatchewan and Montana. Can J Earth Sci 36:717–724
Li L, Keller G (1998) Diversification and extinction in Campanian-Maastrichtian planktic foraminifera of Northwestern Tunisia. Eclog Geol Helv 91:75–102
Lindenmaier F, Stüben D, Kramar U, Stinnesbeck W, Keller G, López-Oliva J-G (1999) Chemostratigraphy of the K/T-boundary at La Sierrita and La Lajilla, NE Mexico. In: Abstracts with Programs. Geological Society of America, Annual Meeting. Denver, Colorado, p 123
López-Ramos E (1975) Geological summary of the Yucatán Peninsula. In: Nairn AEM, Stehli FG (eds) The ocean basins and margins—the Gulf of Mexico and the Caribbean 3. Plenum Press, New York, pp 257–282
Lyons JB, Officer CB (1992) Mineralogy and petrology of the Haiti Cretaceous/Tertiary section. Earth Planet Sci Lett 109:205–224
MacLeod KG, Huber BT (2001) The Maastrichtian record at Blake Nose (western North Atlantic) and implications for global palaeoceanographic and biotic changes. In: Kroon D, Norris RD, Klaus A (eds) Western North Atlantic Paleogene and Cretaceous paleoceanography: Geol Soc Lond Spec Pub 183:111–130
MacLeod N, Rawson PF, Forey PL, Banner FT et al. (1997) The Cretaceous-Tertiary biotic transition. J Geol Soc Lond 154:265–292
Maltman AJ (1994a) The geological deformation of sediments. Chapman and Hall, London
Maltman AJ (1994b) Deformation structures preserved in rocks. In: Maltman AJ (ed) The geological deformation of sediments. Chapman and Hall, London, pp 261–303
Martinez I, Agrinier P, Schärer U, Javoy M (1994) A SEM-ATEM and stable isotope study of carbonates from the Haughton impact crater, Canada. Earth Planet Sci Lett 121:559–574
Martínez-Ruíz F, Ortega-Huertas M, Palomo-Delgado I, Acquafredda P (1997) Quench textures in altered spherules from the Cretaceous-Tertiary boundary layer at Agost and Caravaca, SE Spain. Sediment Geol 113:137–147
Martínez-Ruíz F, Ortega-Huertas M, Palomo-Delgado I, Smit J (2001a) K-T boundary spherules from Blake Nose (ODP Leg 171B) as a record of the Chicxulub ejecta deposits. In: Kroon D, Norris RD, Klaus A (eds) Western North Atlantic Paleogene and Cretaceous paleoceanography. Geol Soc Lond Spec Pub 183:149–161
Martínez-Ruíz F, Ortega-Huertas M, Kroon D, Smit J, Palomo-Delgado I, Rocchia R (2001b) Geochemistry of the Cretaceous-Tertiary boundary at Blake Nose (ODP Leg 171B). In: Kroon D, Norris RD, Klaus A (eds) Western North Atlantic Paleogene and Cretaceous paleoceanography. Geol Soc Lond Spec Pub 183:131–148

Martínez-Ruíz F, Ortega-Huertas M, Palomo-Delgado I, Smit J (2002) Cretaceous-Tertiary boundary at Blake Nose (Ocean drilling Program Leg 171B): A record of the Chicxulub impact ejecta. In: Koeberl C, MacLeod KG (eds) Catastrophic events and mass extinctions: Impacts and beyond. Geol Soc Am Spec Pap 356:189–200

Martinsen OJ (1994) Mass movements. In: Maltman AJ (ed) The geological deformation of sediments. Chapman and Hall, London, pp 127–165

Maurrasse FJ-MR, Sen G (1991) Impacts, tsunamis, and the Haitian Cretaceous-Tertiary boundary layer. Science 252:1690–1693

McHugh CMG, Snyder SW, Miller KG (1998) Upper Eocene ejecta of the New Jersey continental margin reveal dynamics of Chesapeake Bay impact. Earth Planet Sci Lett 160:353–367

Melosh HJ (1989) Impact cratering. Oxford University Press, New York

Mittlefehldt DW, See TH, Hörz F (1992) Dissemination and fractionation of projectile materials in the impact melts from the Wabar Crater, Saudi Arabia. Meteoritics 27:361–370

Montanari A (1991) Authigenesis of impact spheroids in the K/T boundary clay from Italy: New constraints for high-resolution stratigraphy of terminal Cretaceous events. J Sediment Petrol 61:315–339

Montanari A, Koeberl C (2000) Impact stratigraphy lecture notes in Earth sciences 93. Springer, Berlin Heidelberg New York

Moore DM, Reynolds RC (1997) X-ray diffraction and the identification and analysis of clay minerals. Oxford University Press, Oxford

Mørk MBE, Leith DA, Fanavoll S (2001) Origin of carbonate-cemented beds on the Naglfar Dome, Voring Basin, Norwegian Sea. Mar Petrol Geol 18:223–234

Morton RA (1993) Attributes and origins of ancient submarine slides and filled embayments: Examples from the Gulf Coast Basin. AAPG Bull 77:1064–1081

Mulder T, Cochonat P (1996) Classification of offshore mass movements. J Sediment Res 66:43–57

Murray JW (1991) Ecology and palaeoecology of benthic foraminifera. Longman Scientific, London

Newman ACD, Brown G (1987) The chemical constitution of clays. In: Newman ACD (ed) Chemistry of clays and cay minerals. Mineralogical Society Monograph 6. Longman Scientific, London, pp 1–128

Nichols RJ (1995) The liquification and remobilization of sandy sediments. In: Hartley AJ, Prosser DJ (eds) Characterization of deep marine clastic systems. Geol Soc Lond Spec Pub 94:63–76

Norris RD, Firth JV (2002) Mass wasting of Atlantic continental margins following the Chicxulub impact event. In: Koeberl C, MacLeod KG (eds) Catastrophic events and mass extinctions: impacts and beyond. Geol Soc Am Spec Pap 356:79–96

Norris RD, Huber BT, Self-Trail BT (1999) Synchroneity of the K-T oceanic mass extinction and meteorite impact: Blake Nose, western North Atlantic. Geology 27:419–422

Norris RD, Firth J, Blusztain JL, Ravizza G (2000) Mass failure of the North Atlantic margin triggered by the Cretaceous-Paleogene bolide impact. Geology 28:1119–1122

Olsson RK, Miller KG, Browning JV, Habib D, Sugarmann PJ (1997) Ejecta layer at the Cretaceous-Tertiary boundary, Bass River, New Jersey (Ocean Drilling Program Leg 174AX). Geology 25:759–762

Olsson RK, Miller KG, Browning JV, Wright JD, Cramer BS (2002) Sequence stratigraphy and sea-level changes across the Cretaceous-Tertiary boundary on the New Jersey passive margin. In: Koeberl C, MacLeod KG (eds) Catastrophic events and mass extinctions: Impacts and beyond. Geol Soc Am Spec Pap 356:97–108

Ormö J, Lindström M (2000) When a cosmic impact strikes the sea bed. Geol Mag 137:67–80

Ortega-Huertas M, Palomo-Delgado I, Martínez-Ruíz F, Gonzalez I (1998) Geological factors controlling clay mineral patterns across the Cretaceous-Tertiary boundary in Mediterranean and Atlantic sections. Clay Miner 33:483–500

Osinski GR, Spray JG (2001) Impact-generated carbonate melts: evidence from the Haughton structure, Canada. Earth Planet Sci Lett 194:17–29

Pardo A, Ortiz N, Keller G (1996) Latest Maastrichtian and Cretaceous-Tertiary foraminiferal turnover and environmental changes at Agost Spain. In: MacLeod N, Keller G (eds) Cretaceous-Tertiary boundary mass extinction: Biotic and environmental changes. Norton Press, New York, pp 139–171

Philpotts AR (1990) Principles of igneous and metamorphic rocks. Prentice Hall, Englewood Cliffs

Pierazzo E, Kring DA, Melosh HJ (1998) Hydrocode simulations of the Chicxulub impact event and the production of climatically active gases. J Geophys Res 103:28607–28625

Pierazzo E, Melosh HJ (1999) Hydrocode modeling of Chicxulub as an oblique impact event. Earth Planet Sci Lett 165:163–176

Pitakpaivan K, Byerly GR, Hazel JE (1994) Pseudomorphs of impact spherules from a Cretaceous-Tertiary boundary section at Shell Creek, Alabama. Earth Planet Sci Lett 124:49–56

Pollastro RM, Bohor BF (1993) Origin and clay-mineral genesis of the Cretaceous/Tertiary boundary unit, Western Interior of North America. Clays Clay Miner 41:7–25

Pope KO, Baines KH, Ocampo AC, Ivanov BA (1997) Energy, volatile production, and climate effects of the Chicxulub Cretaceous/Tertiary impact. J Geophys Res E102:21645–21664

Pope KO, Ocampo AC, Fischer AG, Alvarez W, Fouke BW, Webster CL, Vega FJ, Smit J, Fritsche AE, Claeys P (1999) Chicxulub impact ejecta from Albion Island, Belize. Earth Planet Sci Lett 170:351–364

Premo WR, Izett GA, Meeker GP (1995) Major-element and isotopic compositions of relic tektites and glass-like shards from the K/T boundary spherule bed at El Mimbral, Mexico (abstract). Lun Planet Sci 26:1139–1140

Robin E, Swinburn NHM, Froget L, Rocchia R, Gayraud J (1996) Characteristics and origin of the glass spherules from the Paleocene flood basalt province of western Greenland. Geochim Cosmochim Acta 60:815–830

Ryder G, Fastovsky D, Gartner S (eds) (1996) The Cretaceous-Tertiary event and other catastrophes in Earth history. Special Paper 307. Geological Society of America, Boulder, Colorado, 556 pp

Schilli L (2000) Etude de la limite K-T dans la région de la Sierrita, Nuevo Leon, Mexique. Unpublished master Thesis, Université de Neuchâtel, 138 pp

Schlager W, Buffler RT, Angstadt D, Phair R (1984) Geologic history of the southeastern Gulf of Mexico. In: Buffler RT, Schlager W, Bowdler JL et al. (eds) Deep Sea Drilling Project, Initial Reports 77. Ocean Drilling Program, College Station, Texas, pp 715–738

Schmitz B (1988) Origin of microlayering in worldwide distributed Ir-rich marine Cretaceous/Tertiary boundary clays. Geology 16:1068–1072

Schmitz B (1992) Chalcophile elements and Ir in continental Cretaceous-Tertiary boundary clays from the Western Interior of the USA. Geochim Cosmochim Acta 56:1695–1703

Schuraytz BC, Sharpton VL, Marín LE (1994) Petrology of impact-melt rocks at the Chicxulub multiring basin, Yucatán, Mexico. Geology 22:868–872

See TH, Wagstaff J, Yang V, Hörz F, McKay GA (1998) Compositional variation and mixing of impact melts on microscopic scales. Meteor Planet Sci 33:937–948

See TH, Galindo C, Golden DC, Yang V, Mittlefehldt DW, Hörz FP (1999) Major-element composition of ballistically dispersed melts from Meteor Crater, AZ (abstract). Lun Planet Sci 30:#1633 (CD-ROM)

Shanmugam G, Lehtonen LR, Straume T, Syversten SE, Hodgkinson RJ, Skibeli M (1994) Slump and debris-flow dominated upper slope facies in the Cretaceous of the Norwegian and Northern North Seas (61–67°N): implications for sand distribution. AAPG Bull 78:910–937

Shelley D (1993) Igneous and metamorphic rocks under the microscope. Chapman and Hall, London

Sigurdsson H, D'Hondt S, Arthur MA, Bralower TJ, Zachos JC, Van Fossen M, Channell JET (1991) Glass from the Cretaceous/Tertiary boundary in Haiti. Nature 349:482–487

Sigurdsson H, Leckie RM, Acton GD (1997) Shipboard scientific party: Caribbean volcanism, Cretaceous/Tertiary impact, and ocean climate history: Synthesis of Leg 165. In: Sigurdsson H, Leckie RM, Acton GD (eds) Proceedings of ODP, Initial Reports. Ocean Drilling Program, College Station, Texas, pp 377–400

Smit J (1999) The global stratigraphy of the Cretaceous-Tertiary boundary impact ejecta. Annu Rev Earth Planet Sci 27:75–113

Smit J, Klaver GT (1981) Sanidine spherules at the Cretaceous/Tertiary boundary indicate a large impact event. Nature 292:47–49

Smit J, Alvarez W, Montanari A, Swinburne N, Van Kempen TM, Klaver GT, Lustenhouwer WJ (1992a) "Tektites" and microkrystites at the Cretaceous-Tertiary boundary: Two strewn fields, one crater? Lun Planet Sci 23:87–100

Smit J, Montanari A, Swinburn NHM, Alvarez W, Hildebrand AR, Margolis SV, Claeys P, Lowrie W, Asaro F (1992b) Tektite-bearing, deep-water clastic unit at the Cretaceous-Tertiary boundary in northeastern Mexico. Geology 20:99–103

Smit J, Alvarez W, Montanari A, Claeys P, Grajales-Nishimura JM (1996) Coarse-grained, clastic sandstone complex at the K/T boundary around the Golf of Mexico: Deposition by tsunami waves induced by the Chicxulub impact? In: Ryder G, Fastovsky D, Gartner S (eds) The Cretaceous-Tertiary boundary event and other catastrophes in Earth history: Geol Soc Am Spec Pap 307:151–182

Soria AR, Liesa CL, Mata MP, Arz JA, Alegret L, Arenillas I, Meléndez A (2001) Slumping and a sandbar deposit at the Cretaceous-Tertiary boundary in the El Tecolote section (northeastern Mexico): an impact-induced sediment gravity flow. Geology 29:231–234

Soria AR, Liesa CL, Mata MP, Arz JA, Alegret L, Arenillas I, Meléndez A (2002) Reply: Slumping and a sandbar deposit at the Cretaceous-Tertiary boundary in the El Tecolote section (northeastern Mexico): an impact-induced sediment gravity flow. Geology 30:383

Stähle V (1972) Impact glasses from the suevite of the Nördlinger Ries. Earth Planet Sci Lett 17:275–293

Stinnesbeck W, Barbarin JM, Keller G, López-Oliva J-G, Pivnik DA, Lyons JB, Officer CB, Adatte T, Graup G, Rocchia R, Robin E (1993) Deposition of channel deposits near the Cretaceous-Tertiary boundary in northeastern Mexico: catastrophic or "normal" sedimentary deposits? Geology 21:797–800

Stinnesbeck W, Keller G, Adatte T, López-Oliva J-G, MacLeod N (1996) Cretaceous-Tertiary boundary clastic deposits in NE Mexico: bolide impact or sea-level lowstand? In: MacLeod N, Keller G (eds) The Cretaceous-Tertiary boundary mass extinction: biotic and environmental events. Norton Press, New York, pp 471–517

Stinnesbeck W, Keller G, Adatte T, Stüben D, Kramar U, Berner Z, Desremeaux C, Molière E (1999) Beloc, Haiti, revisited: multiple events across the KT boundary in the Caribbean. Terra Nova 11:303–310

Stinnesbeck W, Schulte P, Lindenmaier F, Adatte T, Affolter M, Schilli L, Keller G, Stüben D, Berner Z, Kramar U, Burns SJ, López-Oliva J-G (2001) Late Maastrichtian age of spherule deposits in northeastern Mexico: implication for Chicxulub scenario. Can J Earth Sci 38:229–238

Stix J (1991) Subaqueous, intermediate to silicic-composition explosive volcanism: a review. Earth-Sci Rev 31:21–53

Stow DAV, Mayall M (2000) Deep-water sedimentary systems: new models for the 21st century. Mar Petrol Geol 17:125–135

Stow DAV, Reading HG, Collinson JD (1996) Deep seas. In: Reading HG (ed) Sedimentary environments: Processes, facies and stratigraphy. Blackwell, Oxford, pp 395–454

Stroncik NA, Schmincke H-U (2002) Palagonite—a review. Int J Earth Sci 91:680–697

Stüben D, Kramar U, Berner Z, Eckhardt J-D, Stinnesbeck W, Keller G, Adatte T, Heide K (2002) Two PGE anomalies above the Cretaceous/Tertiary boundary at Beloc/Haiti: geochemical context and consequences for the impact scenario. In: Koeberl C, MacLeod KG (eds) Catastrophic events and mass extinctions: impacts and beyond: Geol Soc Am Spec Pap 356:163–188

Sturkell E, Ormö J, Nõlvak J, Wallin Å (2000) Distant ejecta from the Lockne marine-target impact crater, Sweden. Meteor Planet Sci 35:929–936

Sweet AR (2001) Plants, a yardstick for measuring the environmental consequences of the Cretaceous/Tertiary boundary event. Geosci Can 28:127–138

Sweet AR, Braman DR, Lerbekmo JF (1999) Sequential palnyological changes across the composite Cretaceous-Tertiary (K-T) boundary claystone and contiguous strata, western Canada and Montana, USA. Can J Earth Sci 36:743–768

Toon OB, Zahnle K, Morrison D, Turco RP, Covey C (1997) Environmental perturbations caused by the impacts of asteroids and comets. Rev Geophys 35:41–78

Tsikalas F, Gudlaugsson ST, Faleide JI (1998) Collapse, infilling, and postimpact deformation at the Mjolnir impact structure, Barents Sea. Geol Soc Am Bull 110:537–552

Tucker ME, Wright VP (1992) Carbonate sedimentology. Blackwell, Oxford

Utzmann A, Hansteen TH, Schmincke H-U (2002) Trace element mobility during sub-seafloor alteration of basaltic glass from Ocean Drilling Program site 953 (off Gran Canaria). Int J Earth Sci 91:661–679

Verma HC, Upadhyay C, Tripathi A, Tripathi RP, Bhandari N (2002) Thermal decomposition pattern and particle size estimation of iron minerals associated with the Cretaceous-Tertiary boundary at Gubbio. Meteor Planet Sci 37:901–909

Ward WC, Keller G, Stinnesbeck W, Adatte T (1995) Yucatán subsurface stratigraphy: Implications and constraints for the Chicxulub impact. Geology 23:873–876

Wdowiak TJ, Armendarez LP, Agresti DG, Wade ML, Wdowiak YS, Claeys P, Izett GA (2001) Presence of an iron-rich nanophase material in the upper layer of the Cretaceous-Tertiary boundary clay. Meteor Planet Sci 36:123–133

Wignall PB (2001) Large igneous provinces and mass extinctions. Earth-Sci Rev 53:1–33

Yancey TE (1996) Stratigraphy and depositional environments of the Cretaceous/Tertiary boundary complex and basal section, Brazos River, Texas. Gulf Coast Ass Geol Soc Transact 46:433–442